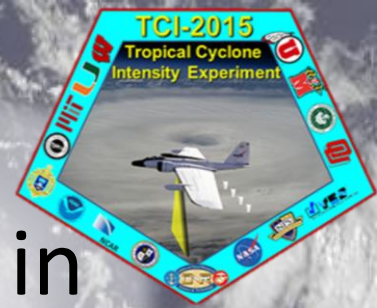




Convective Asymmetries Measured by XDD Dropsondes in Tropical Cyclones

Part I: Joaquin (2015)



***T. Connor Nelson and Lee Harrison
Atmospheric Sciences Research Center
University at Albany, SUNY**

19 August 2016

Goals of Analysis

- Examine the convective updrafts and downdrafts (UDs)
 - Joaquin (2 – 5 October)
- Derive vertical velocity using dropsonde fall speed and density correction
- Evaluate the spatial distribution of abnormally strong UD's (magnitude $\geq 5 \text{ m s}^{-1}$)

Goals of Analysis

- Examine the convective updrafts and downdrafts (UDs)
 - Joaquin (2 – 5 October)
- Derive vertical velocity using dropsonde fall speed and density correction
- Evaluate the spatial distribution of abnormally strong UD's (magnitude $\geq 5 \text{ m s}^{-1}$)

Goals of Analysis

- Examine the convective updrafts and downdrafts (UDs)
 - Joaquin (2 – 5 October)
- Derive vertical velocity using dropsonde fall speed and density correction
- Evaluate the spatial distribution of abnormally strong UD's (magnitude $\geq 5 \text{ m s}^{-1}$)

Methodology

- Compute vertical velocity following similar to Hock and Franklin (1999); however, we use the near surface fall speed instead of drag coefficients:

$$w = V - V_f \quad (1)$$

$$V = (F_o^2) * \sqrt{\frac{\rho_o}{\rho}} \quad (2)$$

$$\rho = \frac{p}{(R_d * T_v)} \quad (3)$$

- Sonde derived vertical velocities were then filtered using a nine-point binomial filter
- UDs were then evaluated based upon thresholds of moderate (magnitude $\geq 5 \text{ m s}^{-1}$), strong (magnitude $\geq 8 \text{ m s}^{-1}$), and extreme (magnitude $\geq 10 \text{ m s}^{-1}$)

Methodology

- Compute vertical velocity following similar to Hock and Franklin (1999); however, we use the near surface fall speed instead of drag coefficients:

$$w = V - V_f \quad (1)$$

$$V = (F_o^2) * \sqrt{\frac{\rho_o}{\rho}} \quad (2)$$

$$\rho = \frac{p}{(R_d * T_v)} \quad (3)$$

- Sonde derived vertical velocities were then filtered using a nine-point binomial filter
- UDs were then evaluated based upon thresholds of moderate (magnitude $\geq 5 \text{ m s}^{-1}$), strong (magnitude $\geq 8 \text{ m s}^{-1}$), and extreme (magnitude $\geq 10 \text{ m s}^{-1}$)

Methodology

- Compute vertical velocity following similar to Hock and Franklin (1999); however, we use the near surface fall speed instead of drag coefficients:

$$w = V - V_f \quad (1)$$

$$V = (F_o^2) * \sqrt{\frac{\rho_o}{\rho}} \quad (2)$$

$$\rho = \frac{p}{(R_d * T_v)} \quad (3)$$

- Sonde derived vertical velocities were then filtered using a nine-point binomial filter
- UDs were then evaluated based upon thresholds of moderate (magnitude $\geq 5 \text{ m s}^{-1}$), strong (magnitude $\geq 8 \text{ m s}^{-1}$), and extreme (magnitude $\geq 10 \text{ m s}^{-1}$)

Methodology

- UDs were restricted to within 1500 km of the TC center and only considered data below 13.5 km
- Used a 'shear-relative' framework
 - DSL = downshear-left, DSR = downshear-right, USL = upshear-left, and USR = upshear-right
 - The environmental shear, TC intensity, and TC heading were obtained from the Statistical Hurricane Intensity Prediction Scheme (SHIPS) dataset (DeMaria and Kaplan 1994)
 - The storm center and radius of maximum wind (RMW) was obtained from the Automated Tropical Cyclone Forecast (AFTC) Best-Track dataset from the National Hurricane Center (NHC)
- The storm center was then linearly interpolated to the minute.

Methodology

- UDs were restricted to within 1500 km of the TC center and only considered data below 13.5 km
- Used a 'shear-relative' framework
 - DSL = downshear-left, DSR = downshear-right, USL = upshear-left, and USR = upshear-right
 - The environmental shear, TC intensity, and TC heading were obtained from the Statistical Hurricane Intensity Prediction Scheme (SHIPS) dataset (DeMaria and Kaplan 1994)
 - The storm center and radius of maximum wind (RMW) was obtained from the Automated Tropical Cyclone Forecast (AFTC) Best-Track dataset from the National Hurricane Center (NHC)
- The storm center was then linearly interpolated to the minute.

Methodology

- UDs were restricted to within 1500 km of the TC center and only considered data below 13.5 km
- Used a 'shear-relative' framework
 - DSL = downshear-left, DSR = downshear-right, USL = upshear-left, and USR = upshear-right
 - The environmental shear, TC intensity, and TC heading were obtained from the Statistical Hurricane Intensity Prediction Scheme (SHIPS) dataset (DeMaria and Kaplan 1994)
 - The storm center and radius of maximum wind (RMW) was obtained from the Automated Tropical Cyclone Forecast (AFTC) Best-Track dataset from the National Hurricane Center (NHC)
- The storm center was then linearly interpolated to the minute

Methodology

- A propensity parameter was calculated

$$\gamma = \frac{n_o}{\frac{H}{F_o} * N} \quad (4)$$

- Spatial Analysis: Polar plots, contoured frequency diagrams by altitude (CFADs), shear-relative azimuth (CFAzDs), and radius (CFRDs)
- Each of the vertical velocity data points that a sonde records were originally assumed to be independent observations
 - One cannot *immediately* ascertain whether any of these data points belong to a single, coherent updraft or a collection of nearby updrafts

Methodology

- A propensity parameter was calculated

$$\gamma = \frac{n_o}{\frac{H}{F_o} * N} \quad (4)$$

- Spatial Analysis: Polar plots, contoured frequency diagrams by altitude (CFADs), shear-relative azimuth (CFAzDs), and radius (CFRDs)
- Each of the vertical velocity data points that a sonde records were originally assumed to be independent observations
 - One cannot *immediately* ascertain whether any of these data points belong to a single, coherent updraft or a collection of nearby updrafts

Methodology

- A propensity parameter was calculated

$$\gamma = \frac{n_o}{\frac{H}{F_o} * N} \quad (4)$$

- Spatial Analysis: Polar plots, contoured frequency diagrams by altitude (CFADs), shear-relative azimuth (CFAzDs), and radius (CFRDs)
- Each of the vertical velocity data points that a sonde records were originally assumed to be independent observations
 - One cannot *immediately* ascertain whether any of these data points belong to a single, coherent updraft or a collection of nearby updrafts

Date	Storm	I [m s ⁻¹]	N _t	S [m s ⁻¹]	S _D [deg]
2 Oct	Joaquin	56.59	75	4.90	151
3 Oct	Joaquin	66.88	65	13.20	127
4 Oct	Joaquin	43.73	66	4.90	66
5 Oct	Joaquin	38.58	76	3.90	39
TOTAL	-----	51.44 (avg)	282	6.73 (avg)	-----

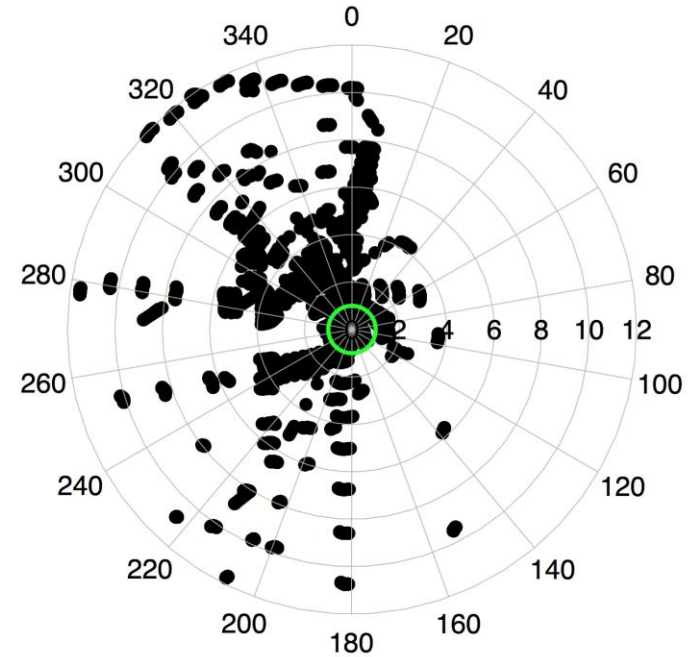
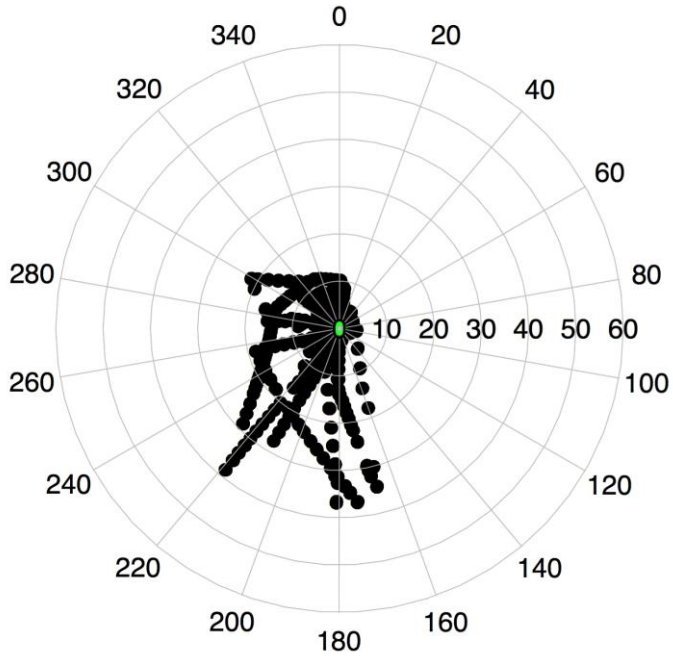
- 282 Sondes Total
- Previous studies of sonde calculated vertical velocities achieve this in many storms (e.g., Stern et al. 2016)
- With ~700 data points per sonde, that's approximately 197,000 data points



Date	Storm	I [m s^{-1}]	N_t	S [m s^{-1}]	S_D [deg]
2 Oct	Joaquin	56.59	75	4.90	151
3 Oct	Joaquin	66.88	65	13.20	127
4 Oct	Joaquin	43.73	66	4.90	66
5 Oct	Joaquin	38.58	76	3.90	39
TOTAL	-----	51.44 (avg)	28	6.73 (avg)	-----

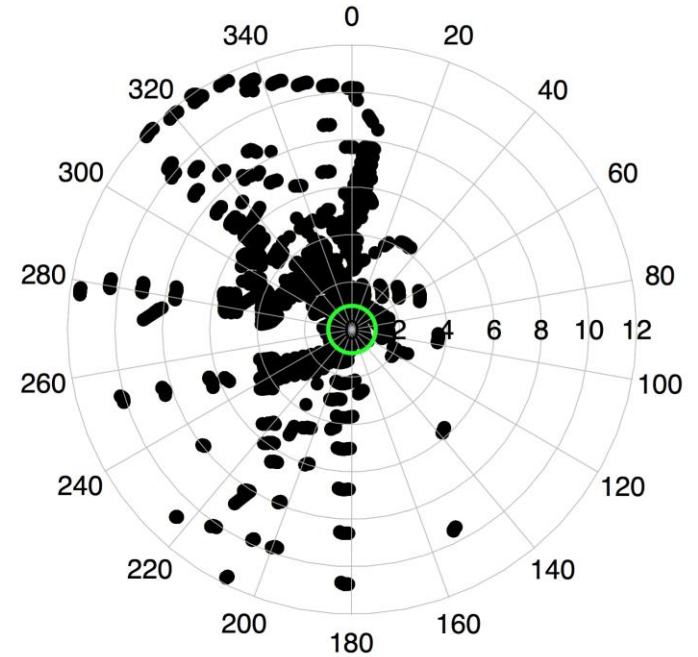
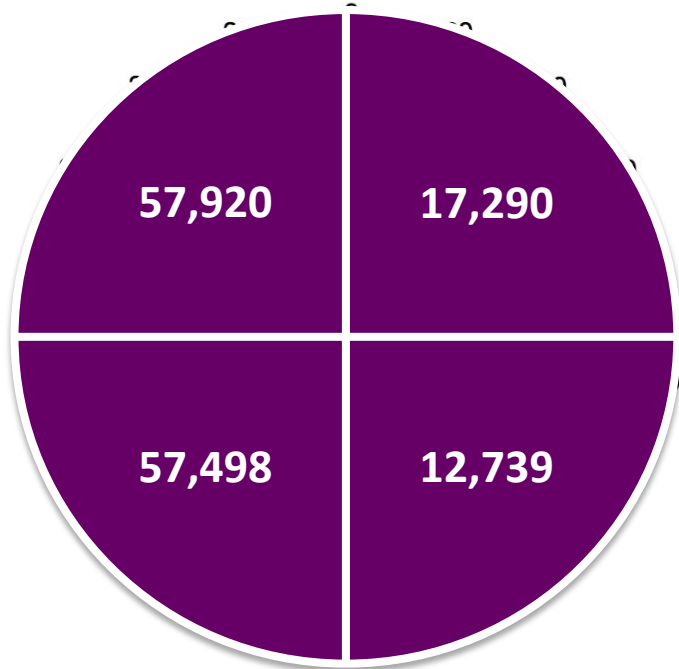
- Moderately sheared
- Maximum observed strength = Cat. 4
- Northwesterly to Southwesterly shear

Spread of Data Points



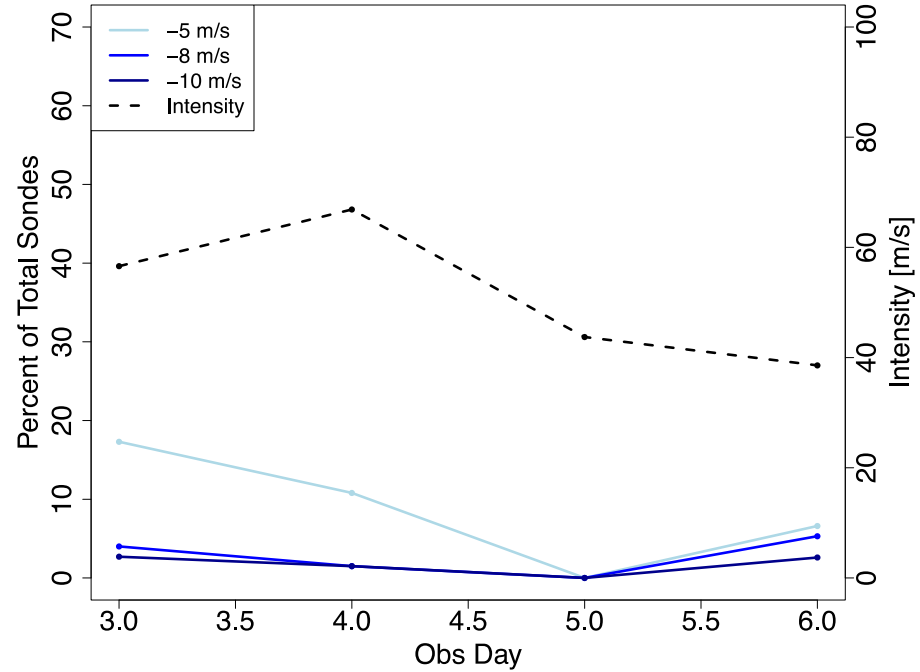
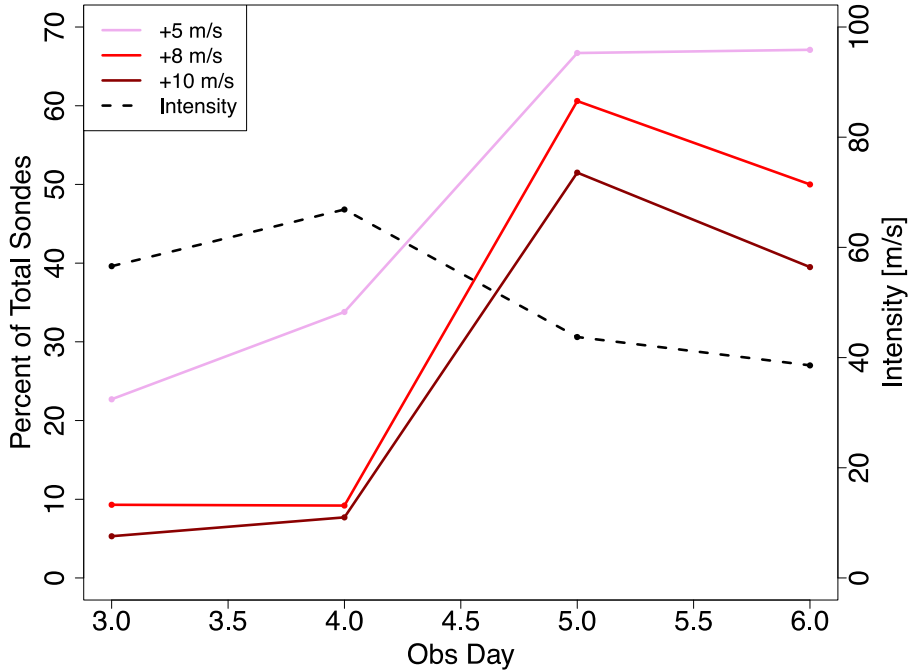
- Great coverage inside $R^* = 2$
- Outside $R^* = 2$, preference for DSL and USL quadrants
 - Void in outer R^* values in DSR

Spread of Data Points

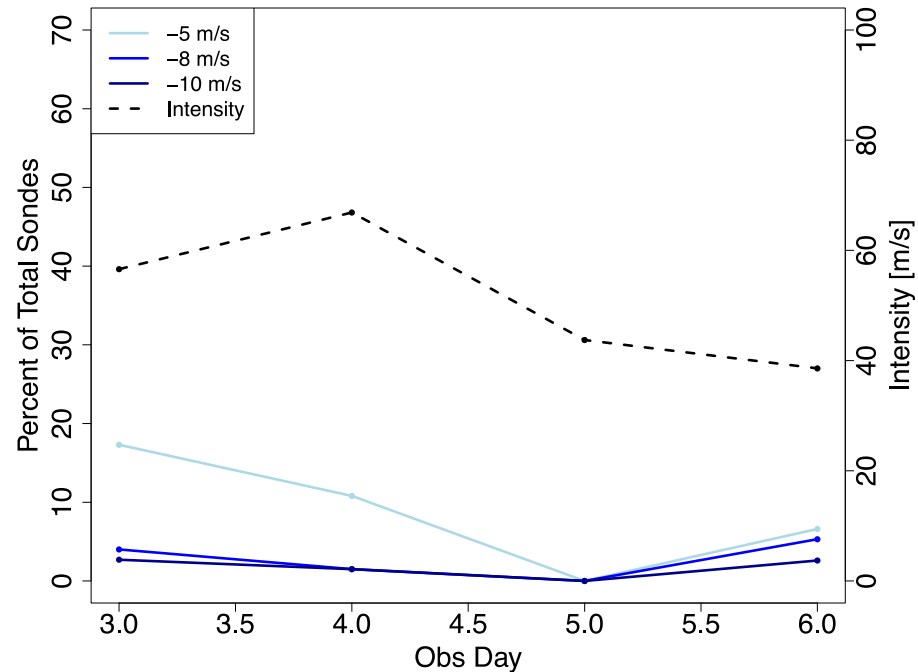
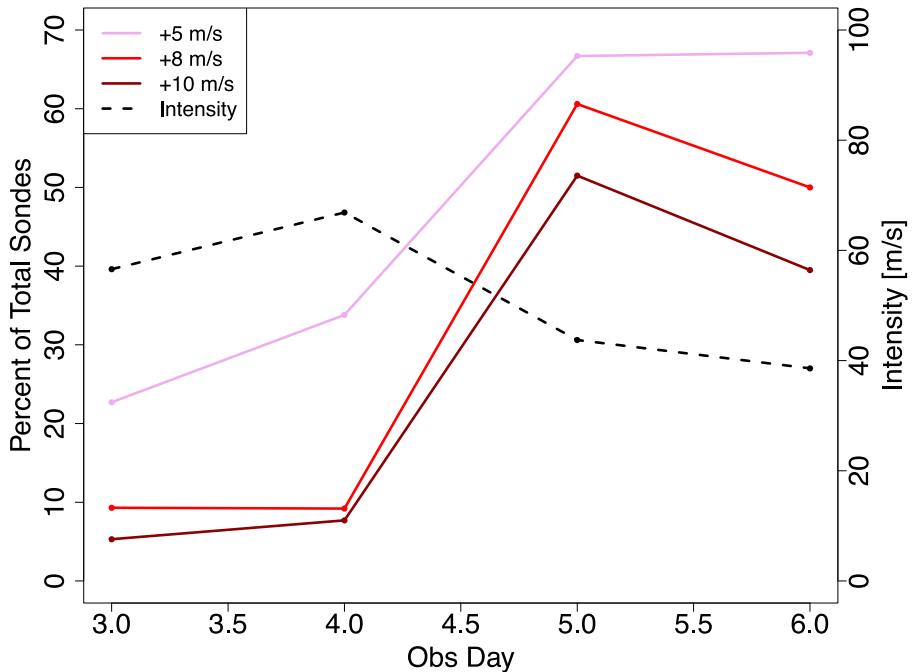


- Definite sampling shear asymmetry
- Will have to be taken into account

Percent of Total Sondes above Threshold

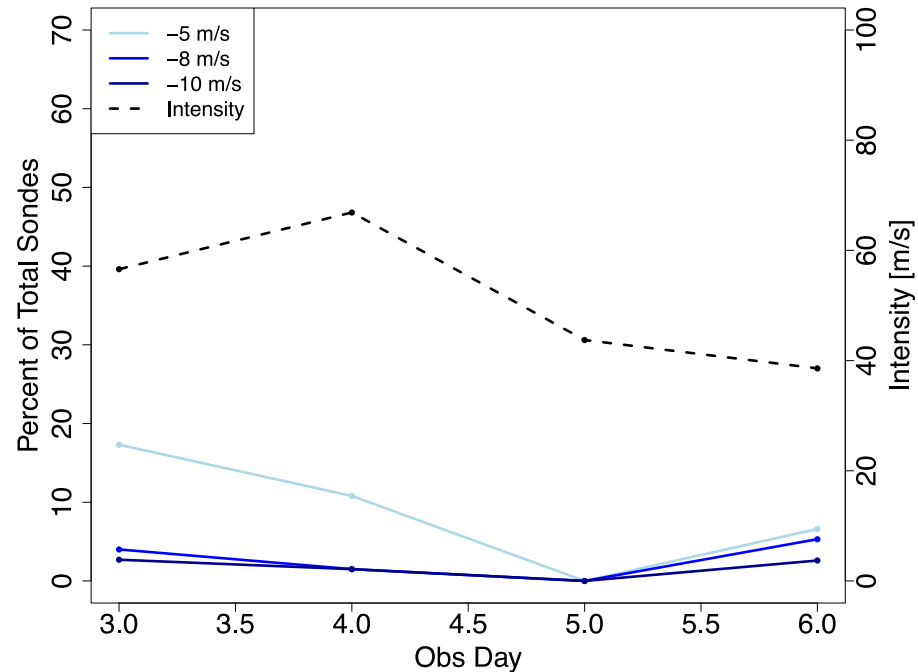
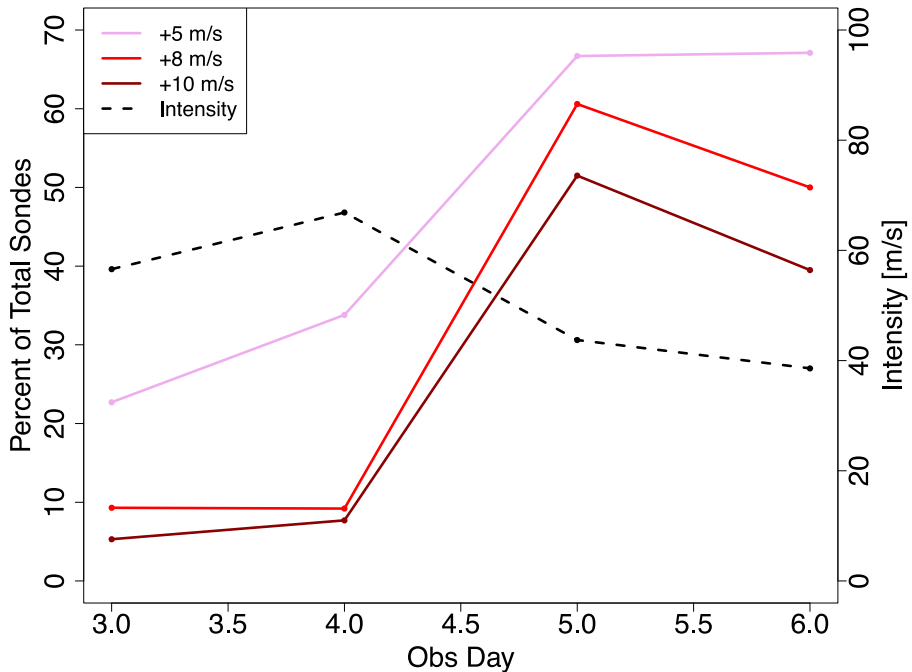


Percent of Total Sondes above Threshold



- Increase of percent of updraft sondes during decay
- Decrease of downdraft sondes after peak intensity
- Maximum Correlations: Positive: +8 m s⁻¹ at -0.89
Negative: - 5 m s⁻¹ at 0.61

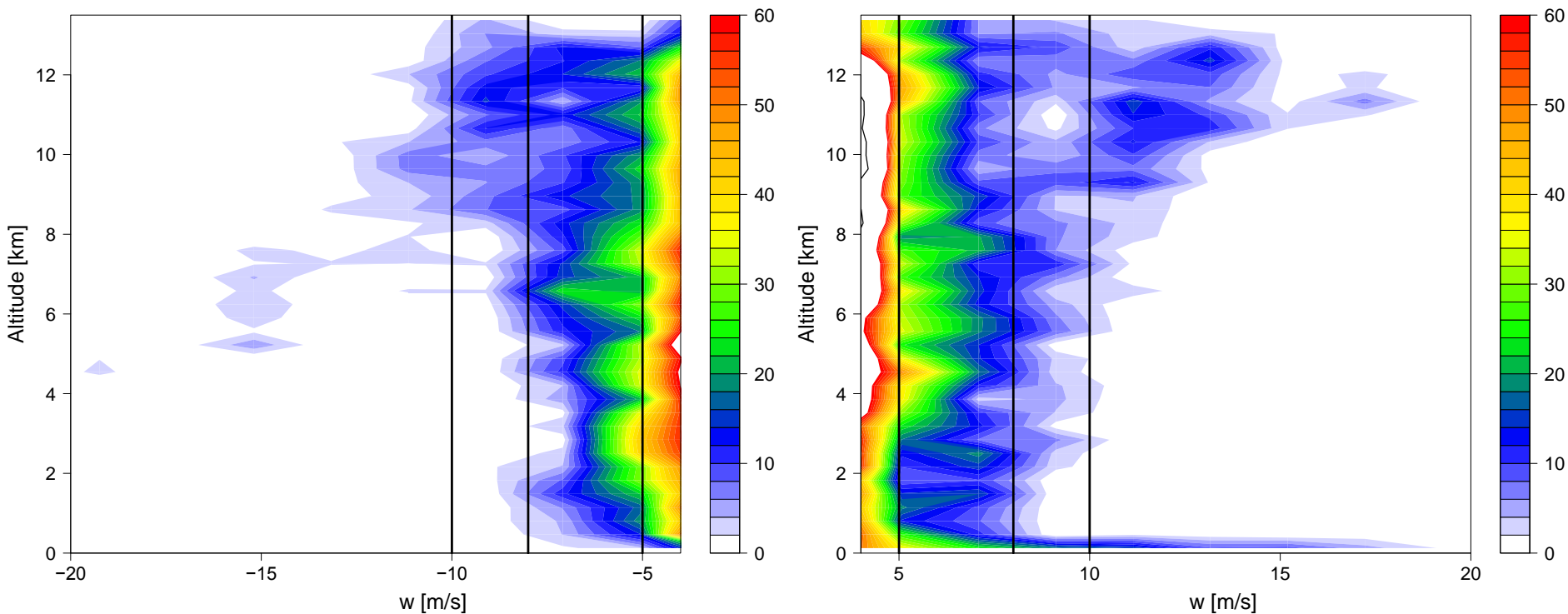
Percent of Total Sondes above Threshold



- Increase of percent of updraft sondes during decay
- Decrease of downdraft sondes after peak intensity
- Maximum Correlations: Positive: $+8 \text{ m s}^{-1}$ at -0.89
Negative: -5 m s^{-1} at 0.61
- Shear –percent correlations slightly weaker

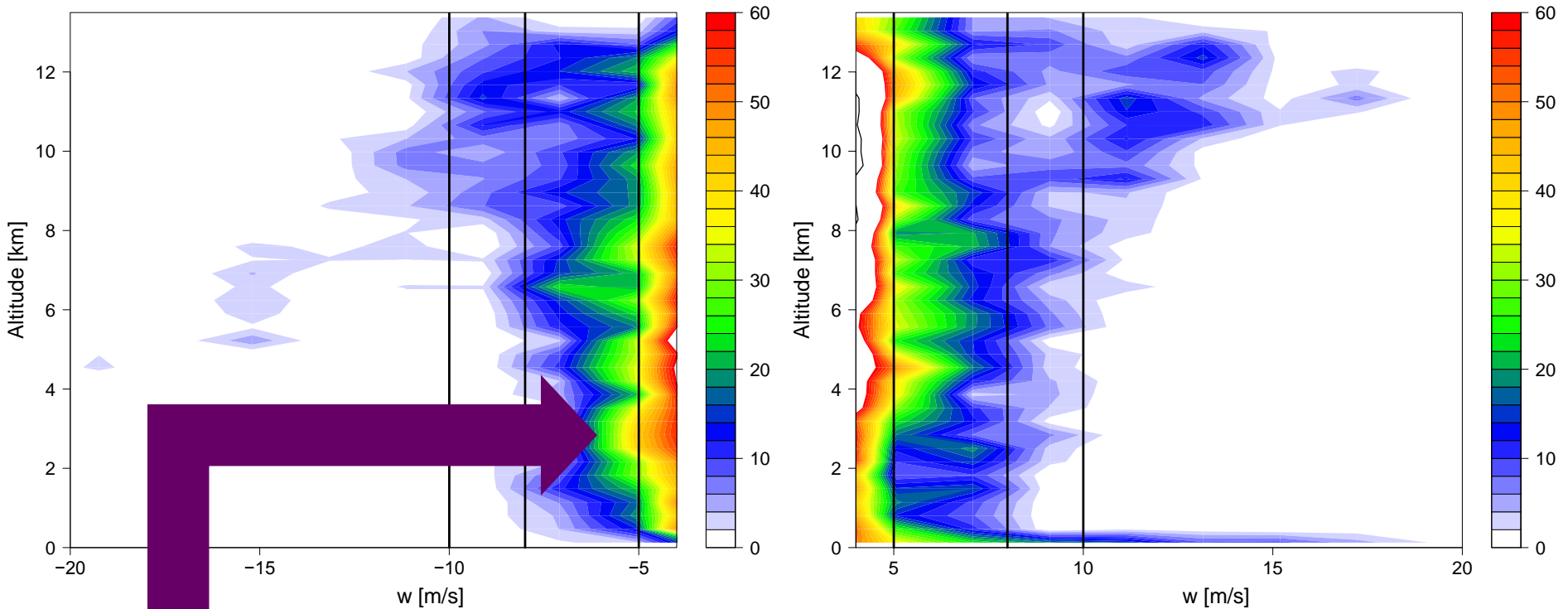
Results: CFADs

Joaquin (2 – 5 October 2015)



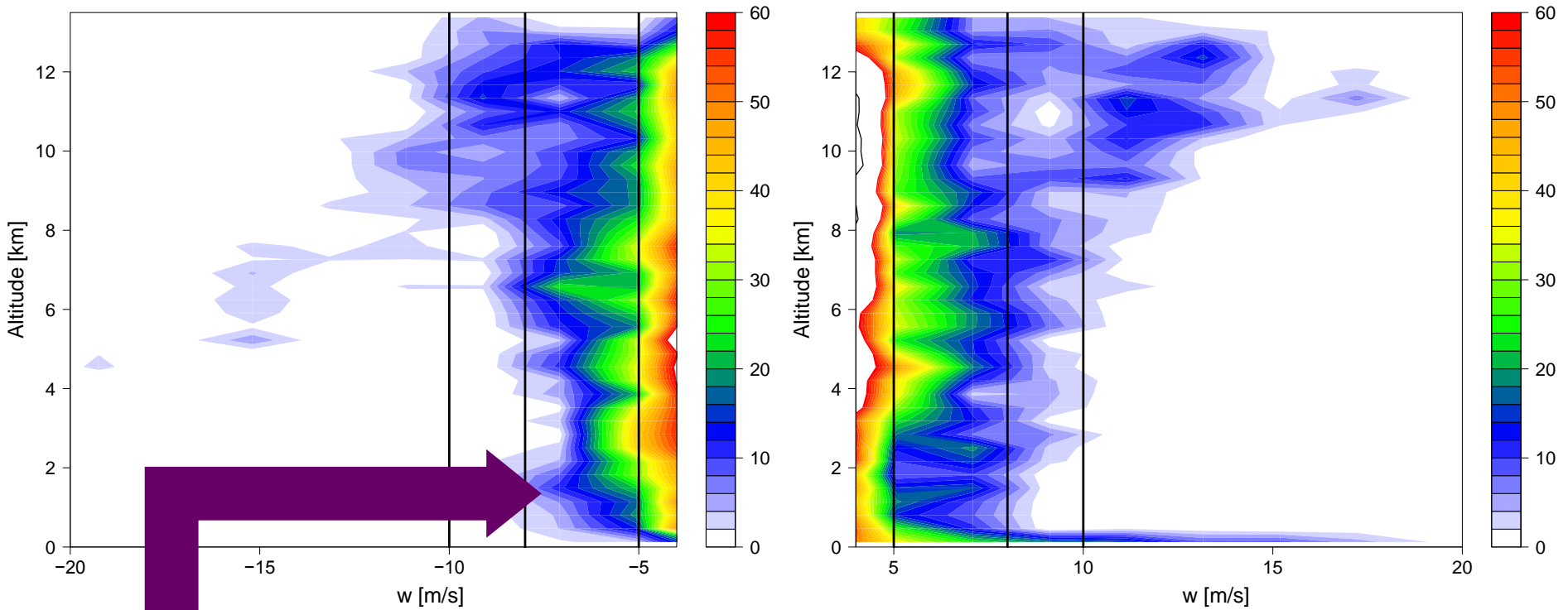
- Moderately sheared ($\sim 7 \text{ m s}^{-1}$)
- Maximum intensity = 66.88 m s^{-1} (Cat. 4)

Joaquin (2 – 5 October 2015)



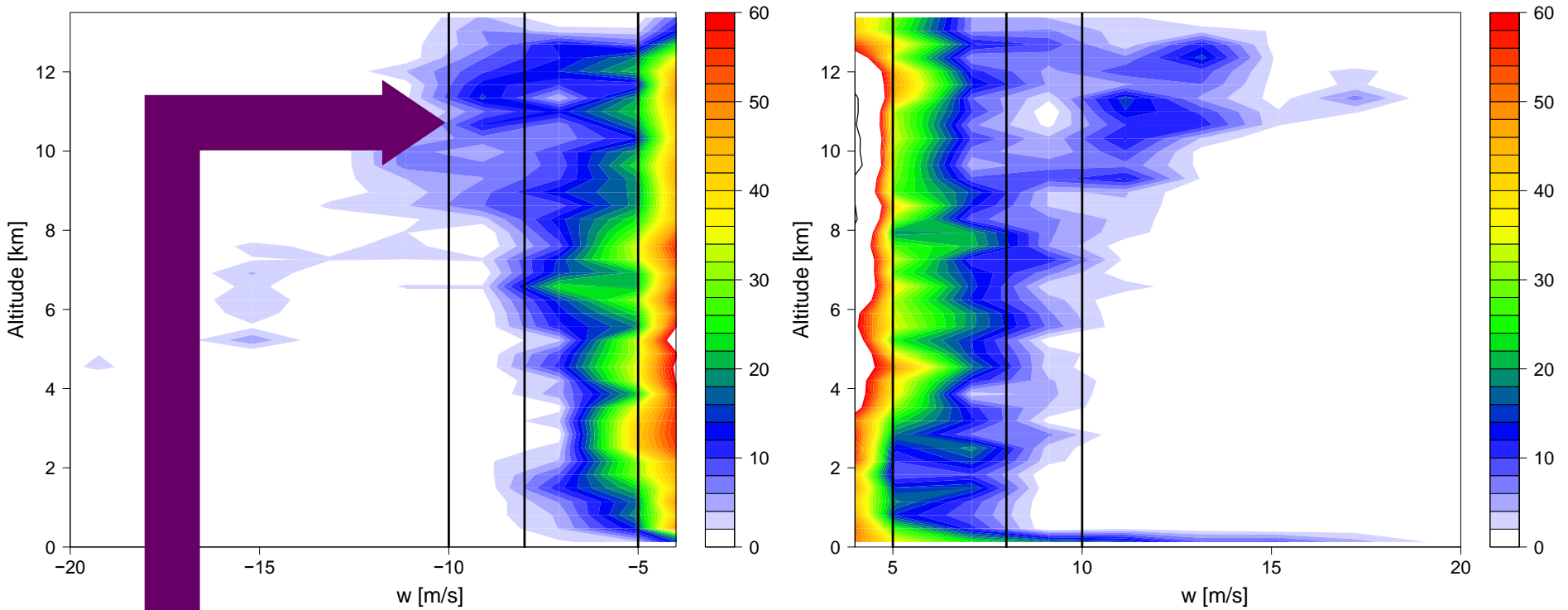
- $> -5 \text{ m s}^{-1}$ tended to occur in mid- and low-levels
- Moderate downdrafts had a single mode at 2.5 km altitude

Joaquin (2 – 5 October 2015)



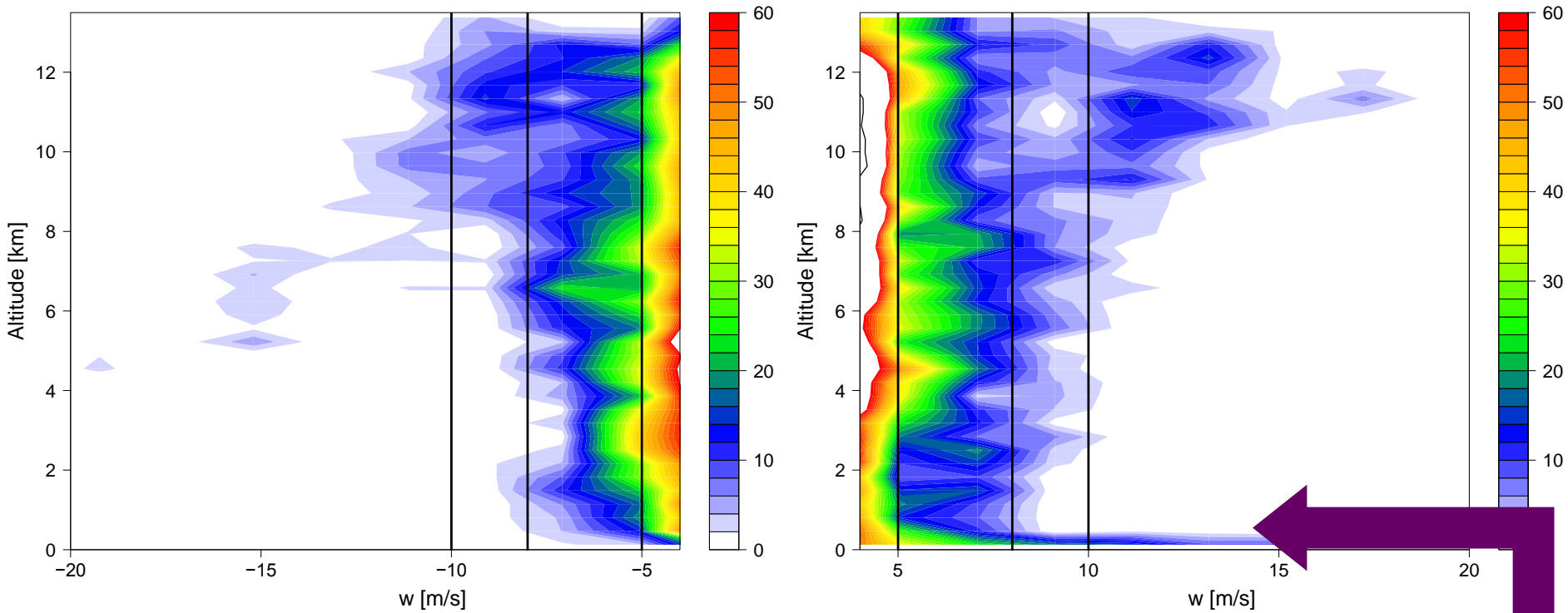
- Small nose below 2 km for strong downdrafts

Joaquin (2 – 5 October 2015)



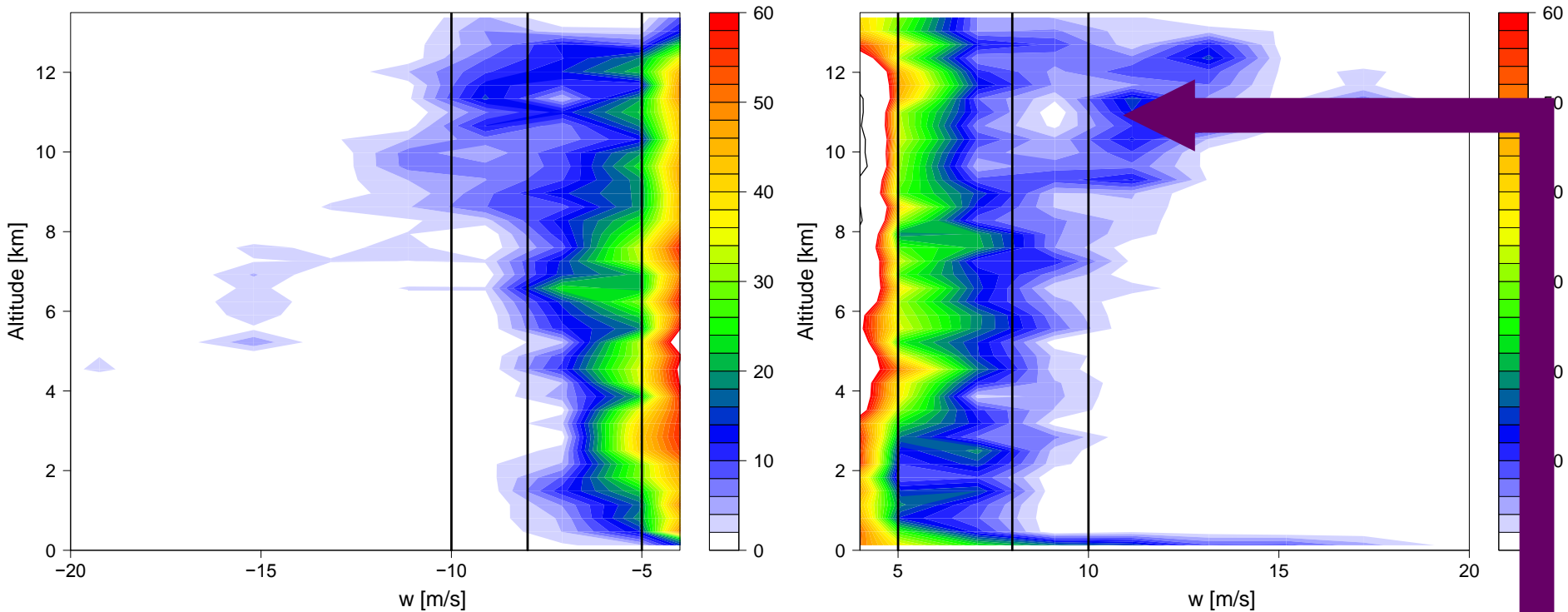
- Strong downdrafts tended to occur aloft up to -11 m s^{-1}
- $< -11 \text{ m s}^{-1}$ altitude decrease

Joaquin (2 – 5 October 2015)



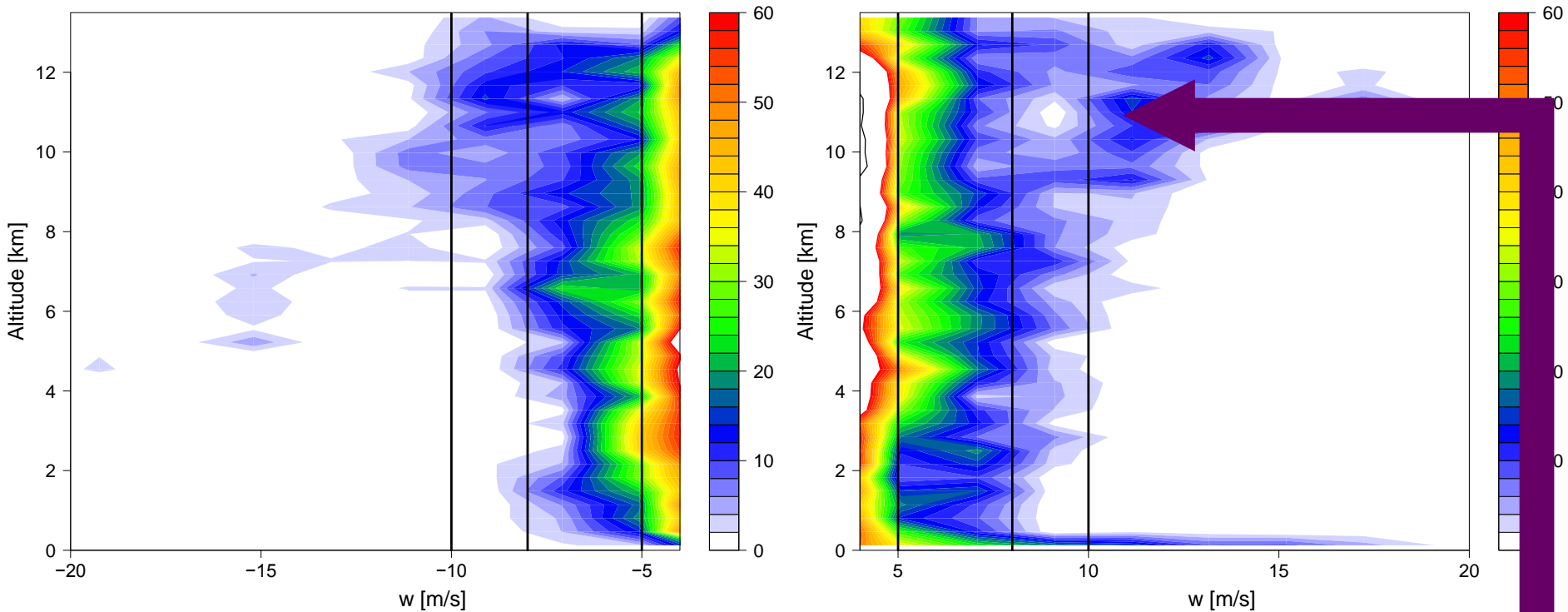
- Presence of near-surface vertical velocity maxima (Stern et al. 2016)

Joaquin (2 – 5 October 2015)



- Higher frequencies for updrafts, stronger
- Above the surface, frequency of updrafts above strong threshold increased with altitude

Joaquin (2 – 5 October 2015)

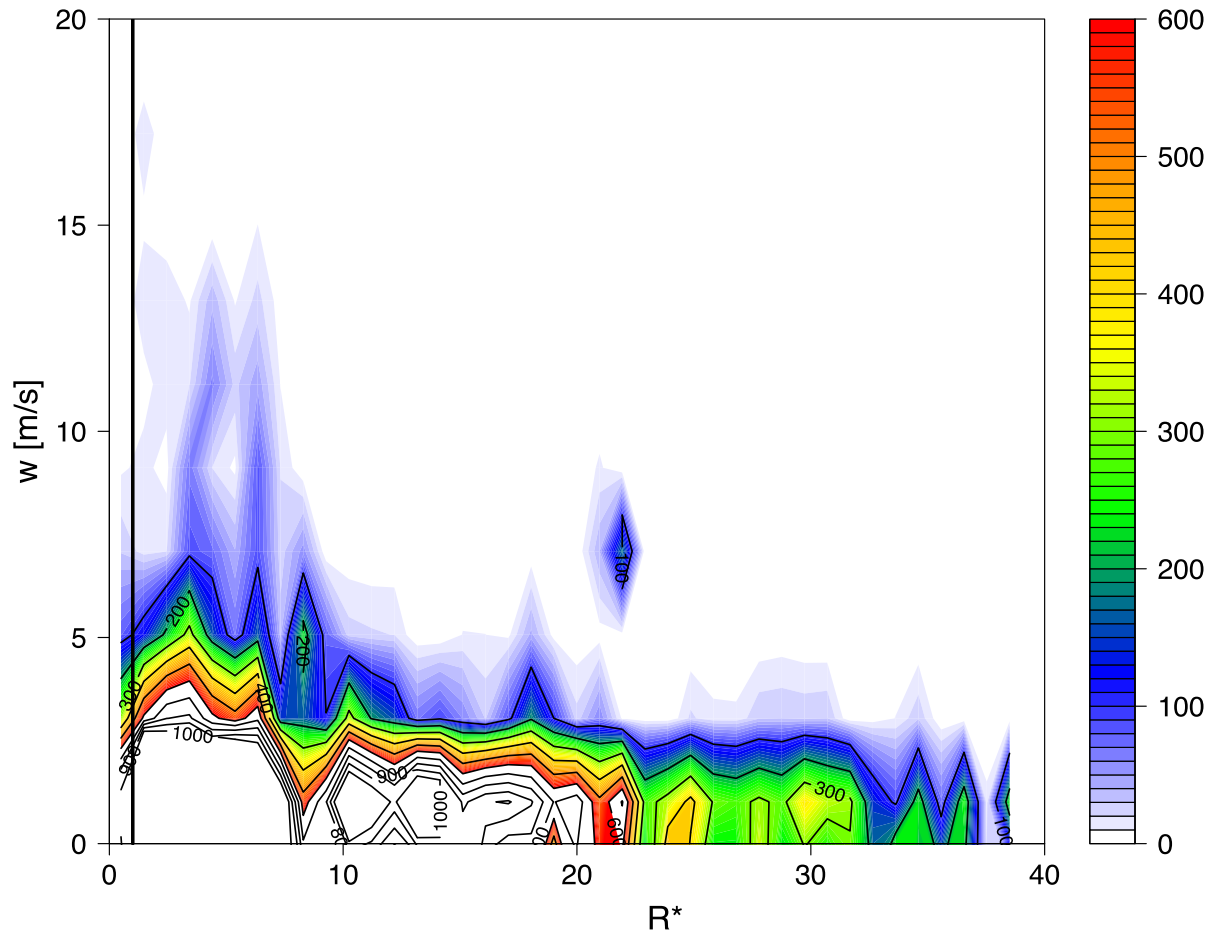


- Extreme updrafts peaked in frequency aloft
- Mid-level maxima for strong updrafts
- Bimodal for moderate updrafts
 - Also, below 5 m s^{-1}

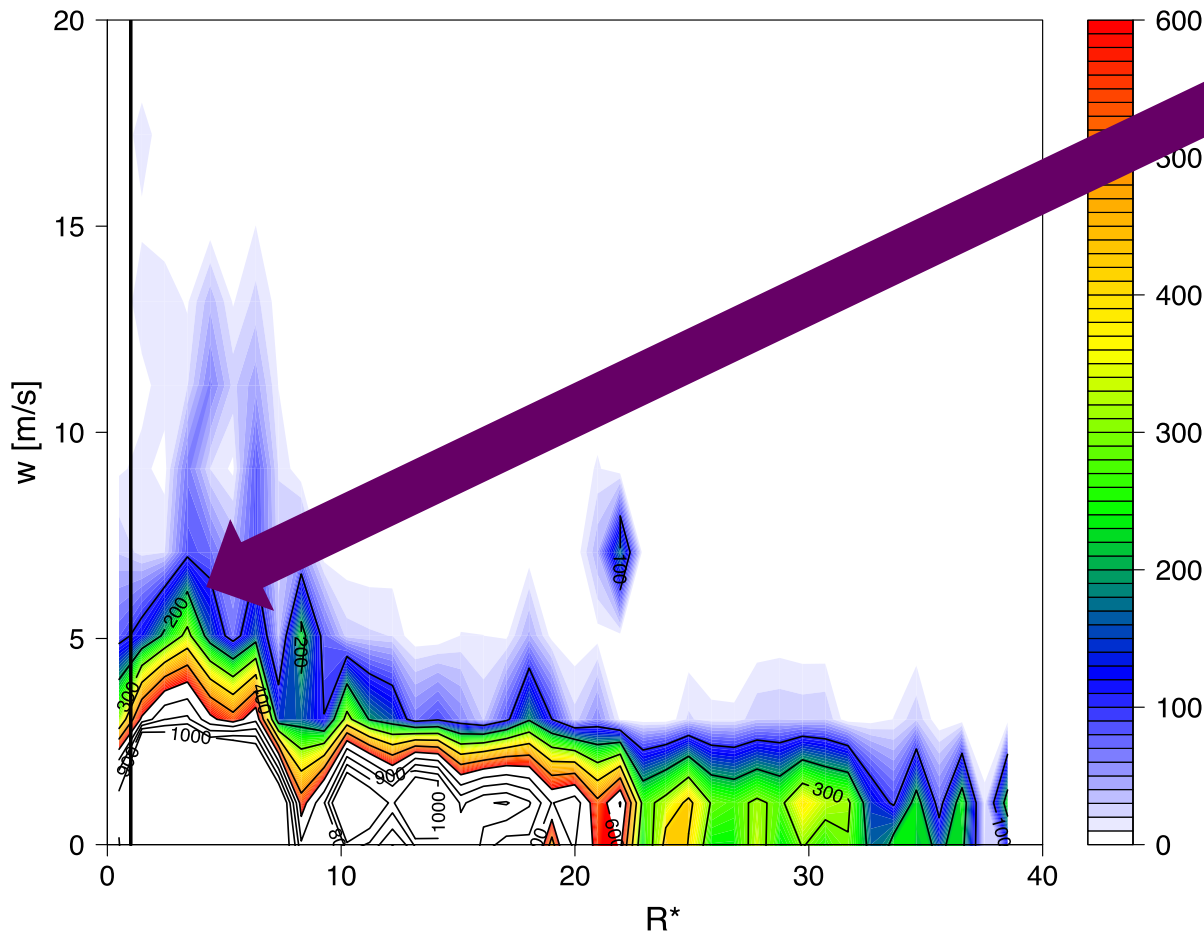
Results: CFRDs*

* For updrafts only

Joaquin (2 – 5 October 2015)

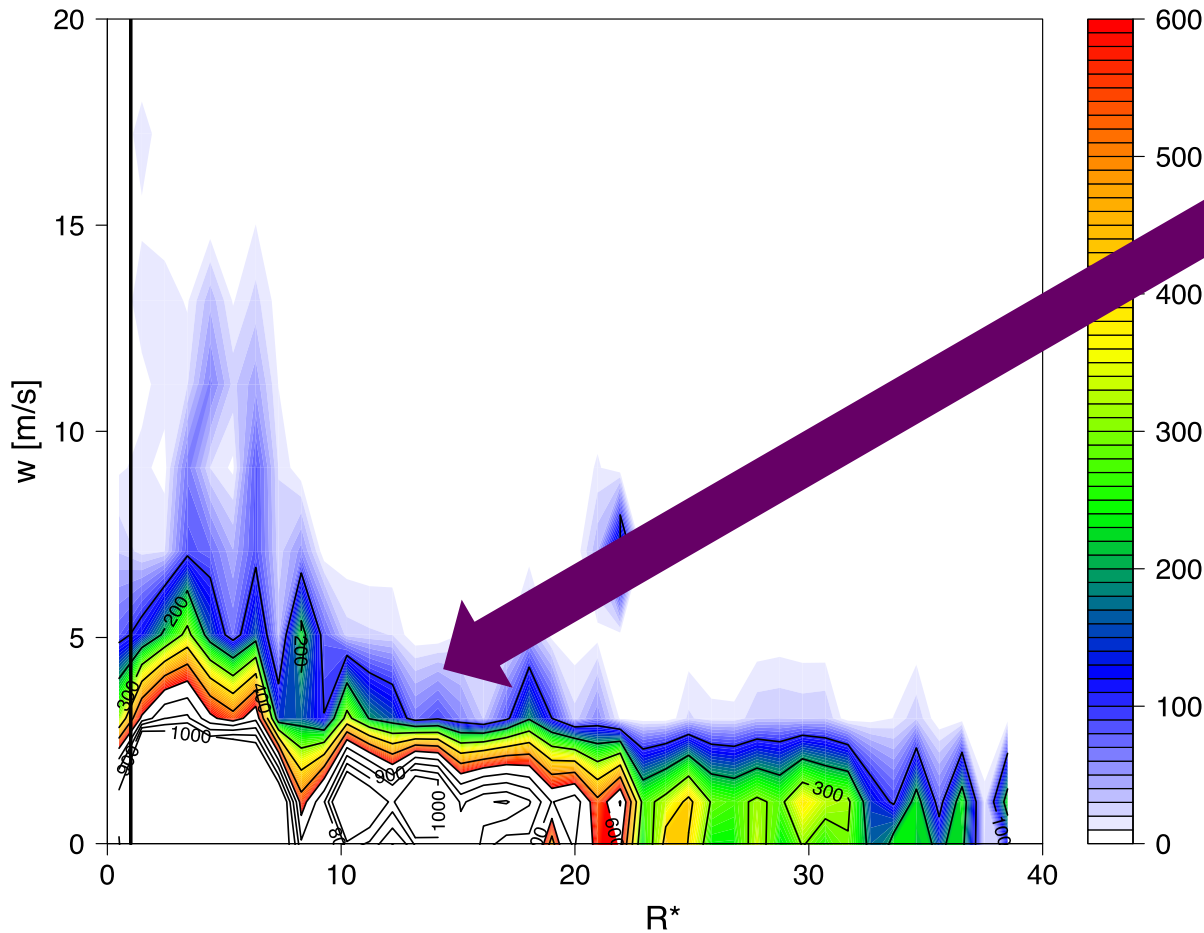


Joaquin (2 – 5 October 2015)



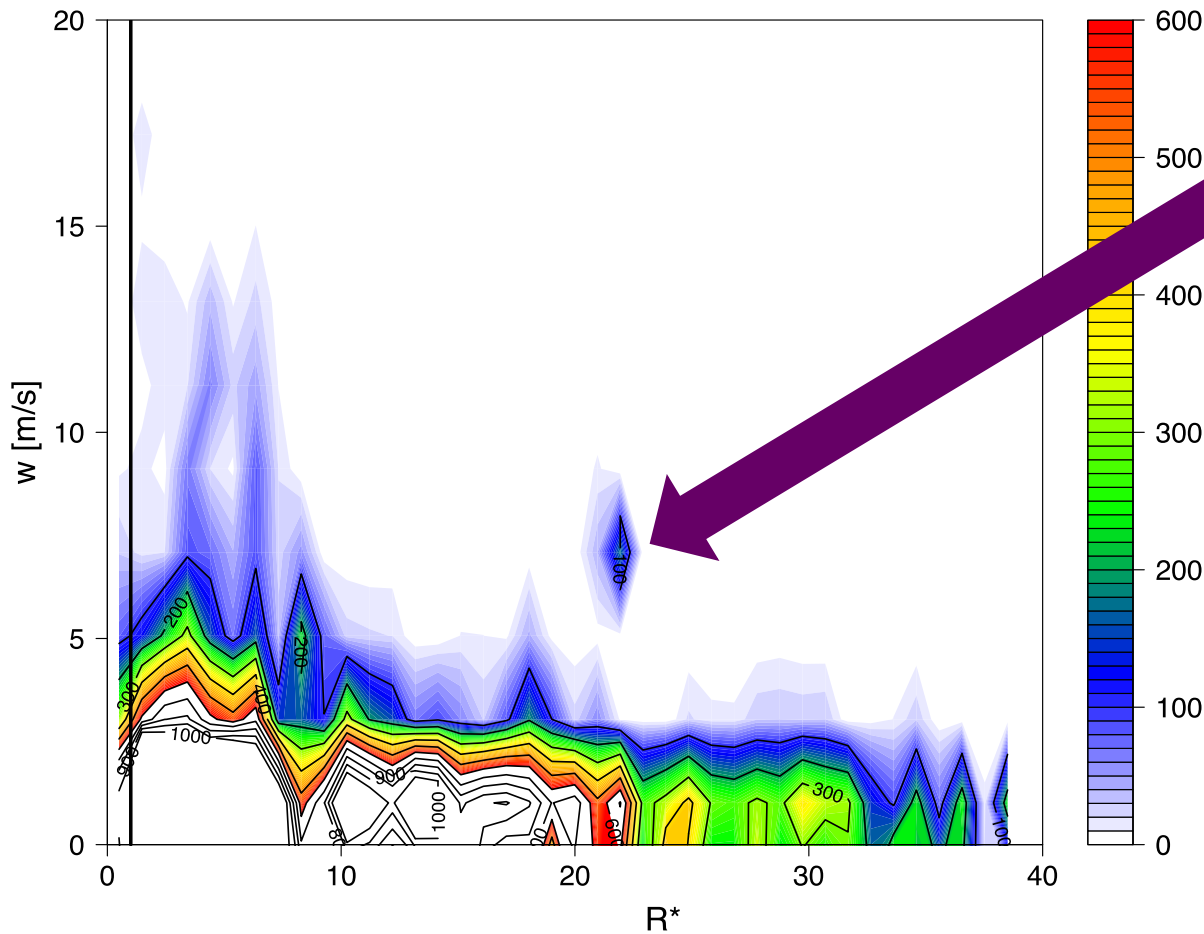
- Sharp increase at the average RMW
- Maximum vertical velocity tended to decrease with radius
- Broad maximum below 5 m s^{-1} over the inner core
- Most updrafts stronger than 5 m s^{-1} were outside the RMW at $R^* = 3$

Joaquin (2 – 5 October 2015)



- Banded features evident with higher frequency lobes out to $R^* = 30$
- Updrafts in rainbands much weaker

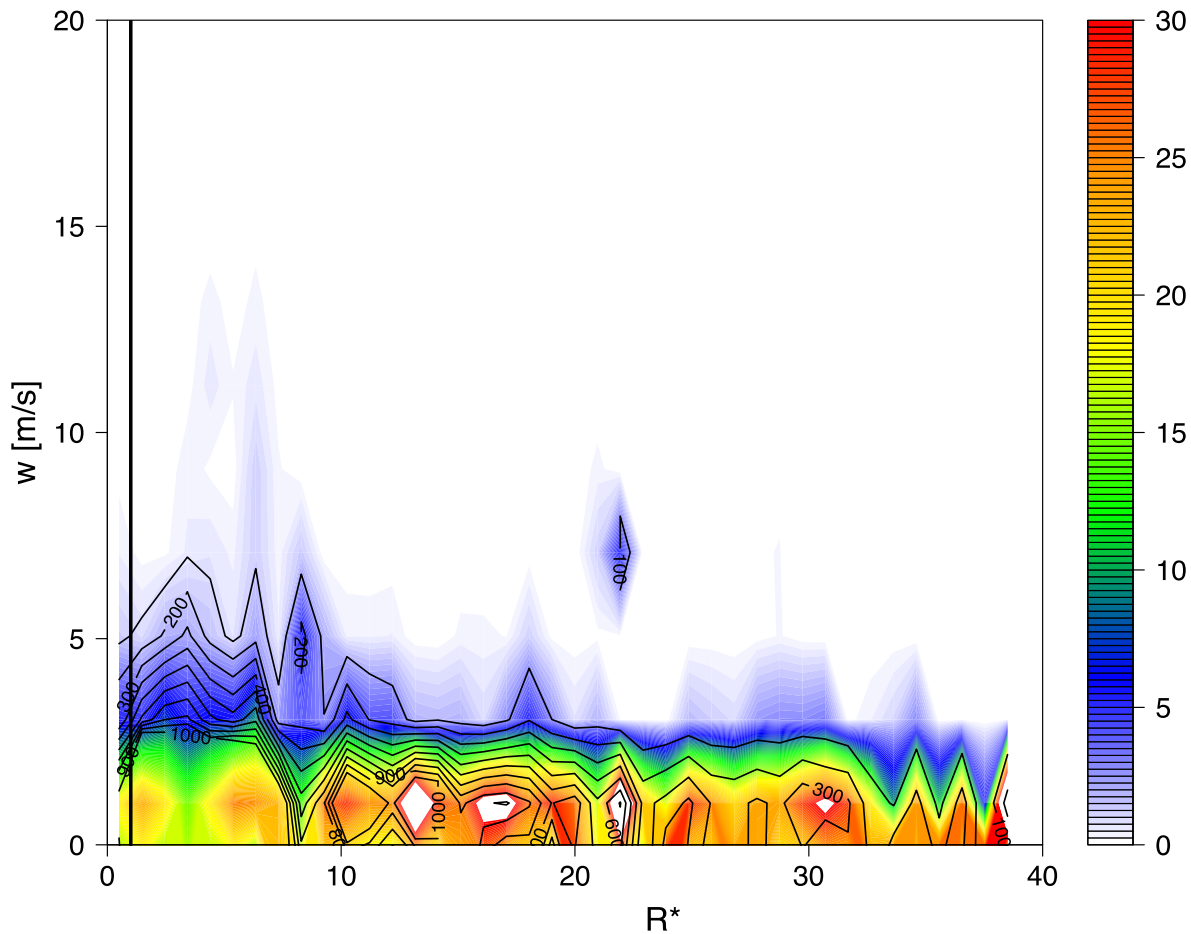
Joaquin (2 – 5 October 2015)



- Unusual isolated lobe of high vertical velocity at $R^* = 22$
 - Corresponds to 800 km peak

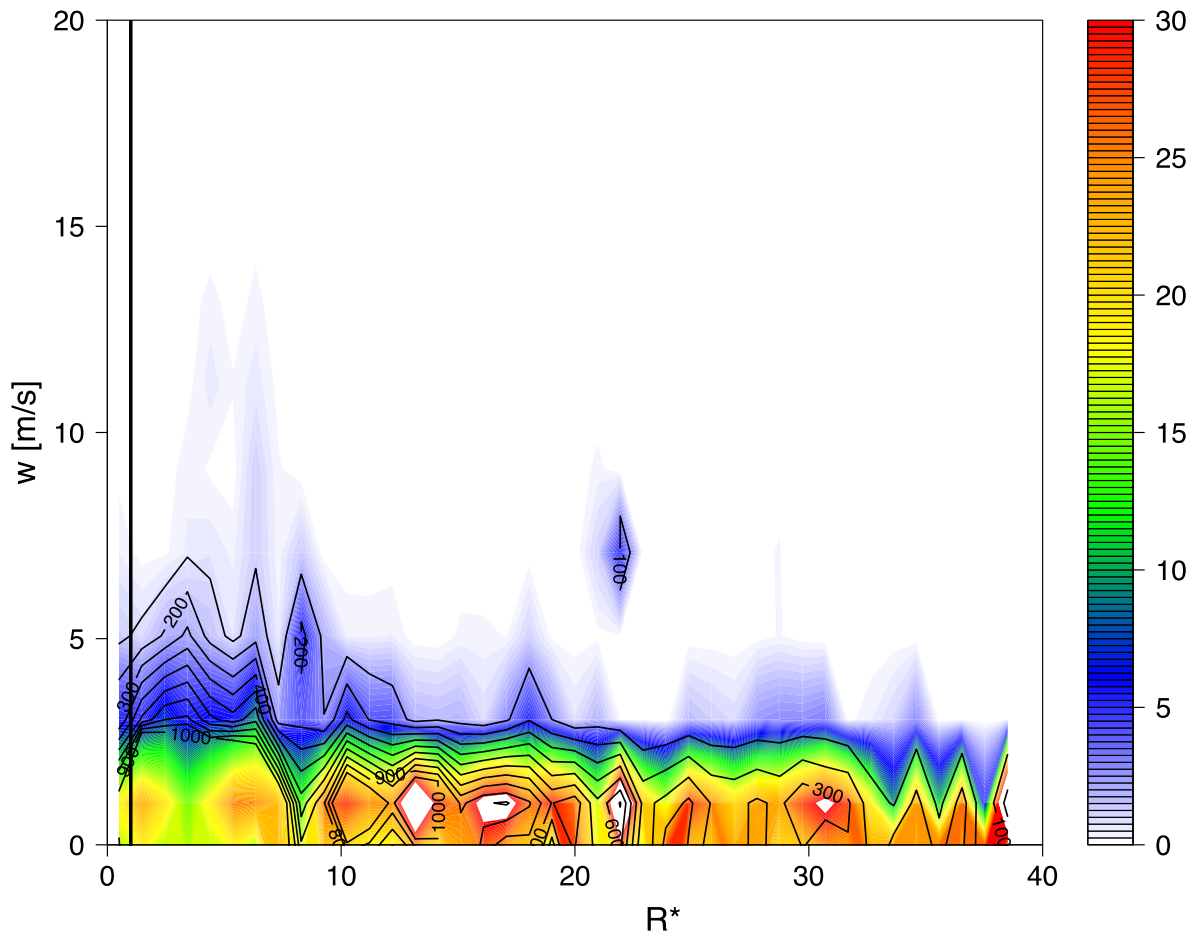
Joaquin (2 – 5 October 2015)

Percentages



Joaquin (2 – 5 October 2015)

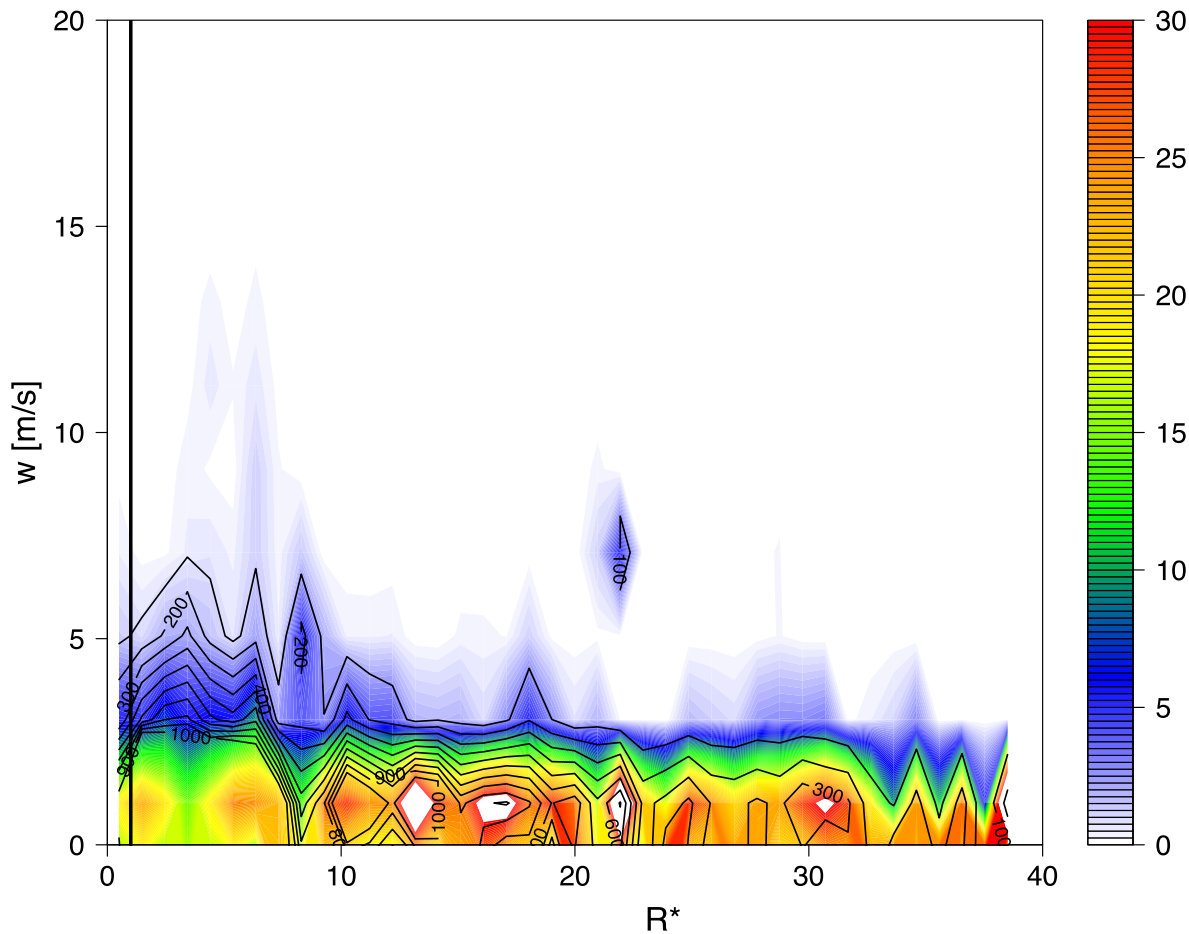
Percentages



- Divide the number of data points in each vertical velocity and radial bin by the total number of data points in each radial bin
 - Sums up to 100% for vertical velocities from -20 m s^{-1} to $+20 \text{ m s}^{-1}$
- Black contours are frequency in intervals of 100 from previous slide

Joaquin (2 – 5 October 2015)

Percentages

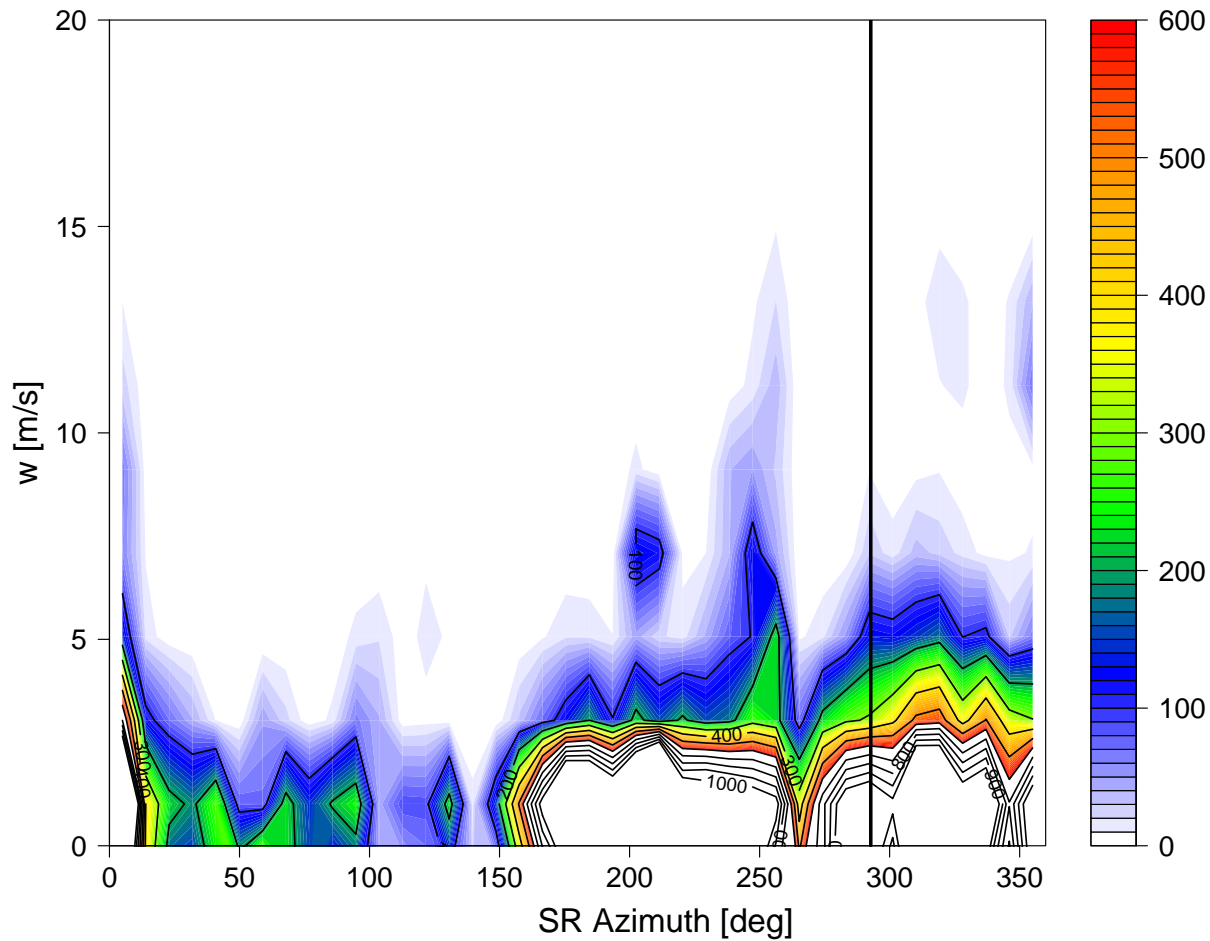


- Still see a decrease in vertical velocity maxima with increasing radius outside of the inner core
- Unexpected point at $R^* = 22$ still there

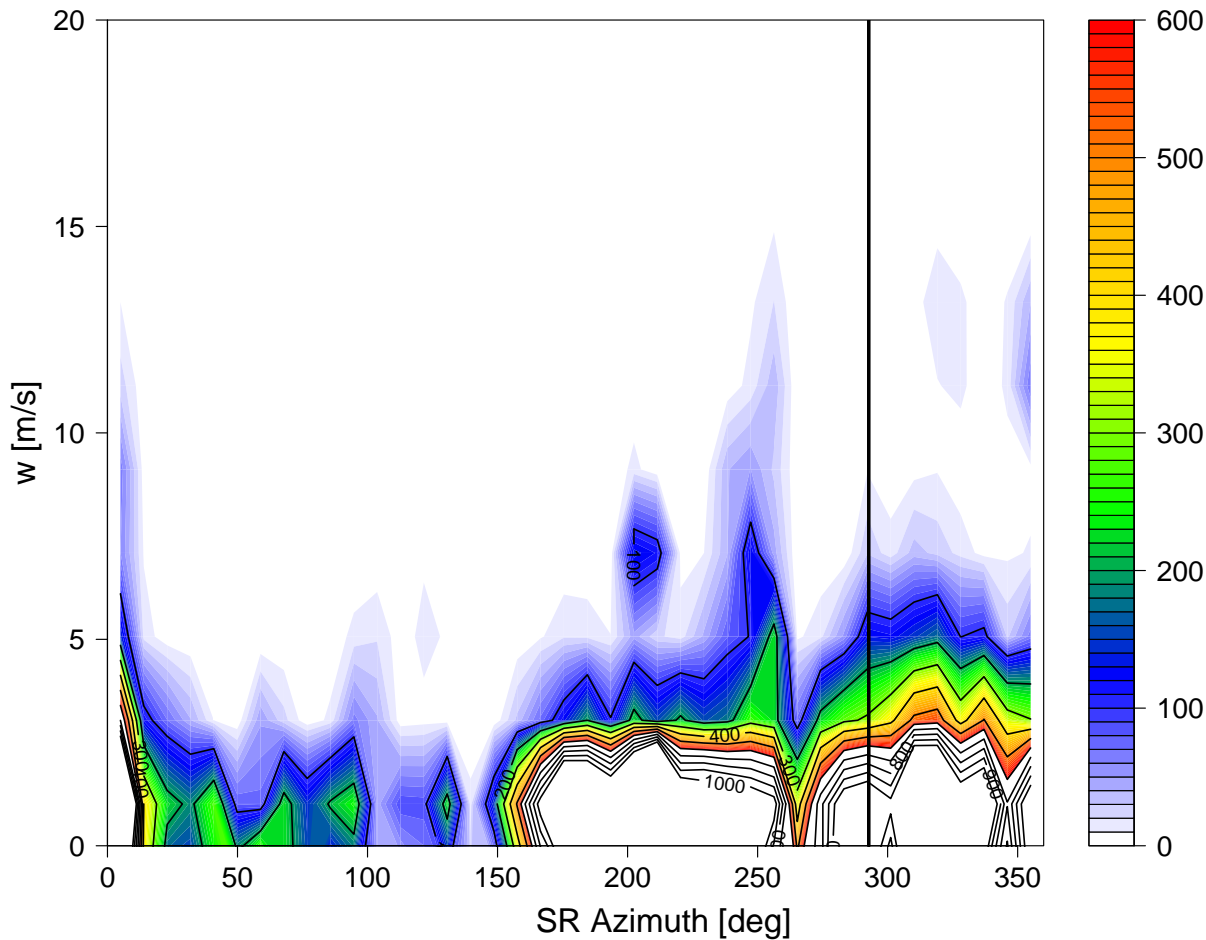
Results: CFAzDs*

* For updrafts only

Joaquin (2 – 5 October 2015)

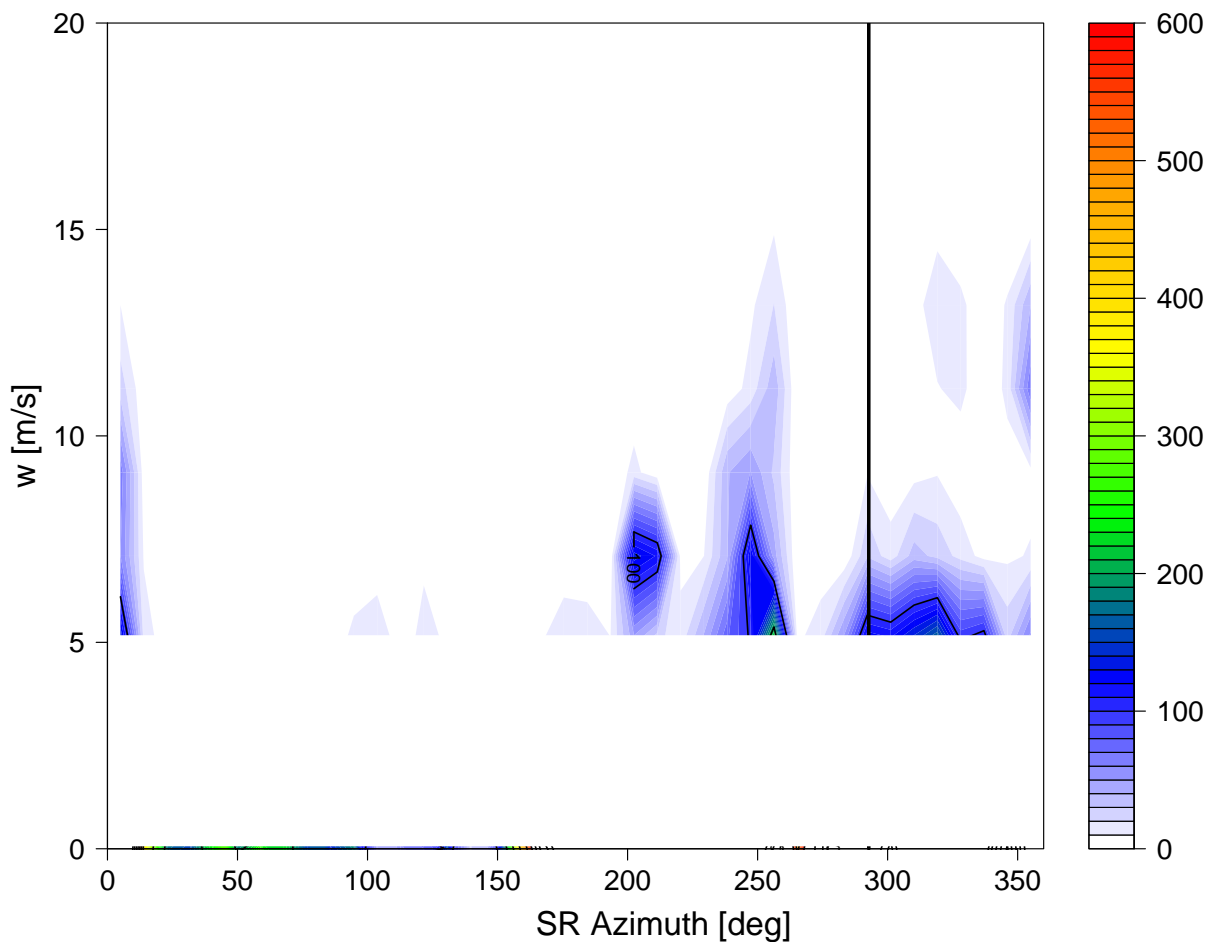


Joaquin (2 – 5 October 2015)



- Frequency maxima in left of shear
- Updrafts stronger than moderate threshold mainly between 200 and 360°
- Suppressed convection in USR (?)

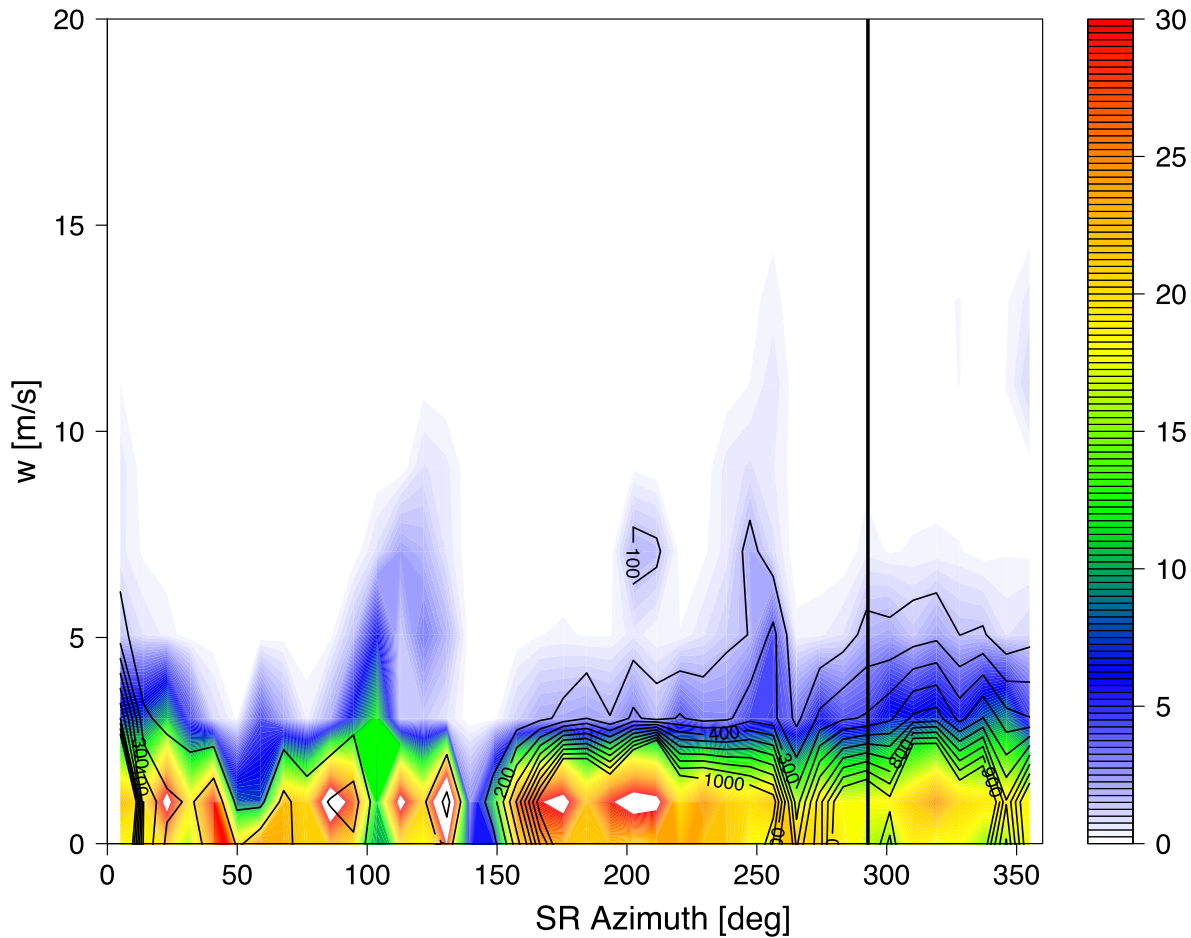
Joaquin (2 – 5 October 2015)



- Looking at just above the moderate threshold:
 - Convective suppression in DSR and USR
 - Convective maxima in downshear

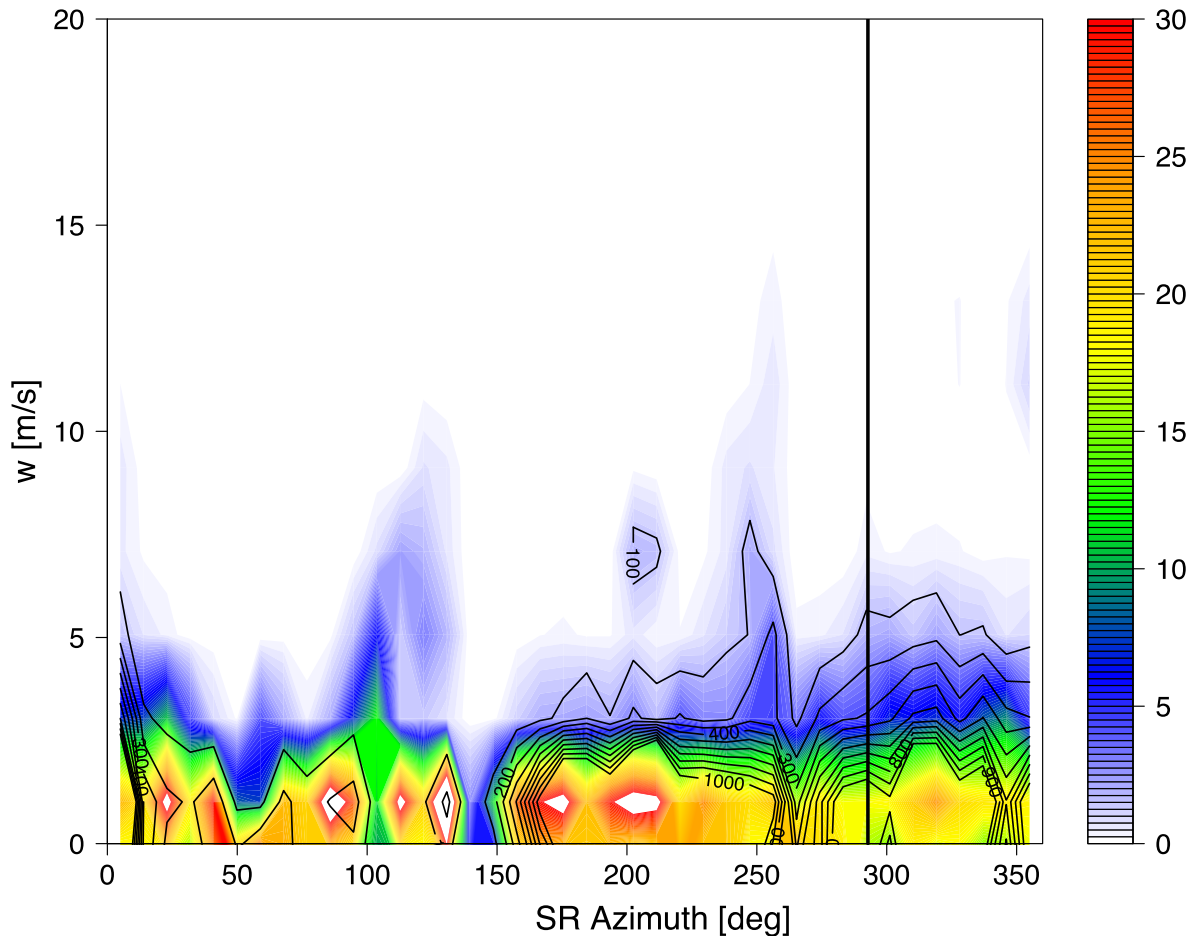
Joaquin (2 – 5 October 2015)

Percentages



Joaquin (2 – 5 October 2015)

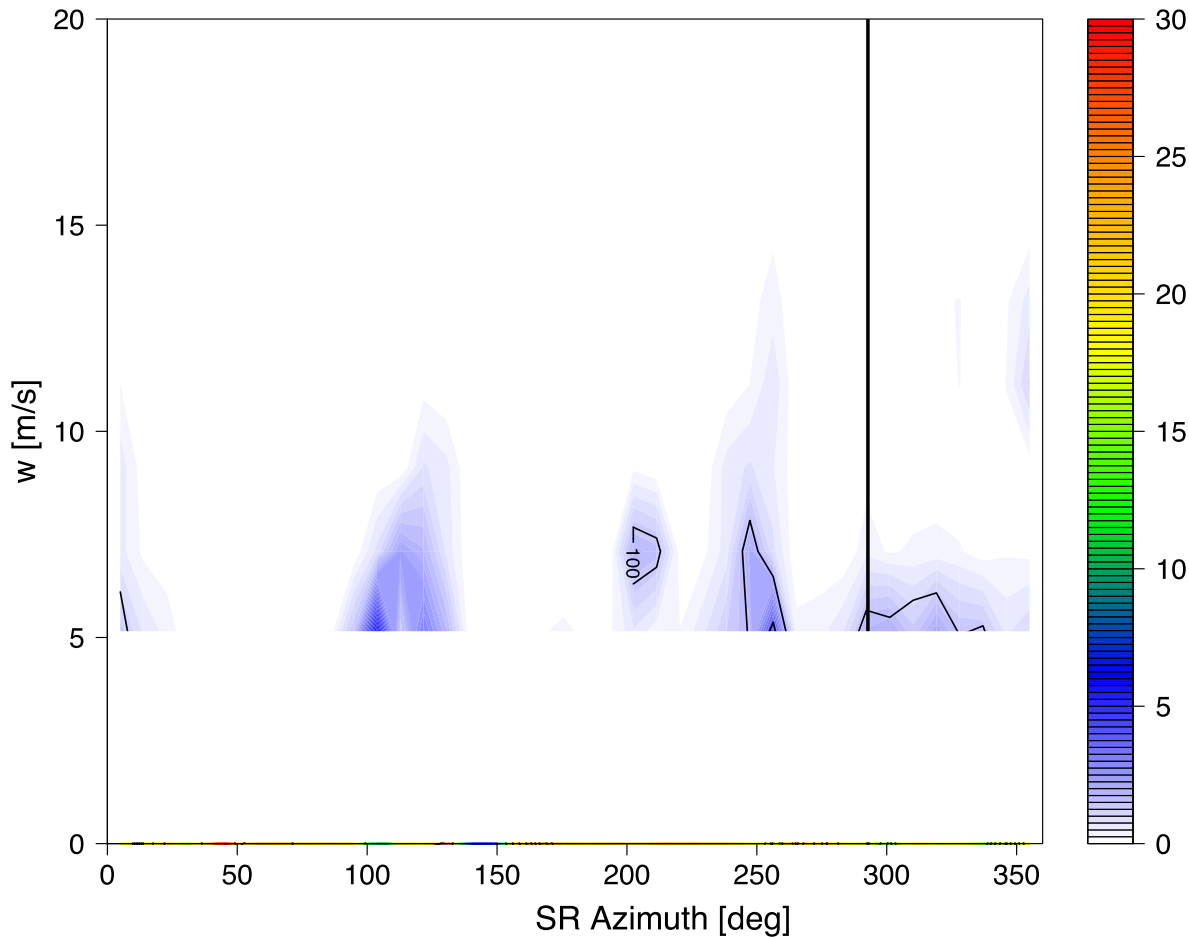
Percentages



- Broad nose of stronger updrafts in the DSL
- Sharp peaks of stronger updrafts in the USL and USR
- Convective suppression near 50 and 150°

Joaquin (2 – 5 October 2015)

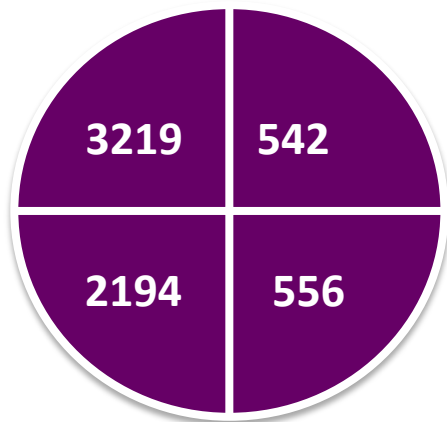
Percentages



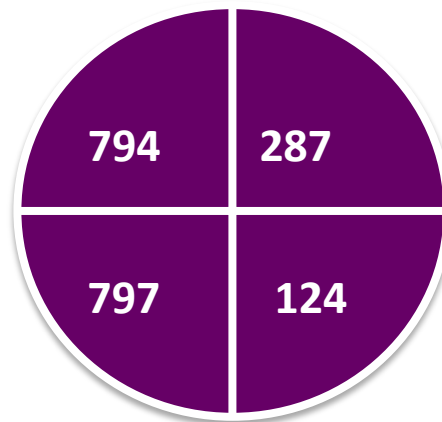
- Looking at just above the moderate threshold:
 - Convective suppression in DSR and USR (only 140—180°)
 - Sharp peak in USR dominates

Updrafts + Downdrafts

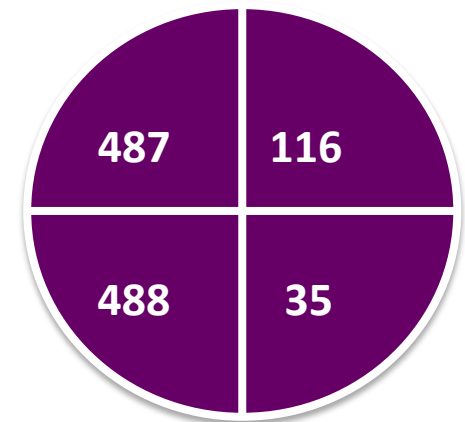
> 5 m s^{-1}



> 8 m s^{-1}



> 10 m s^{-1}



- Moderate convection occurred mainly in the DSL quadrant with a secondary maxima in the USL. Strong and extreme convection maximized in the USL quadrant with a secondary maxima in the DSL

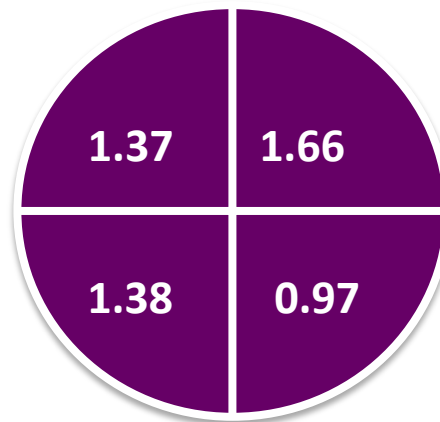
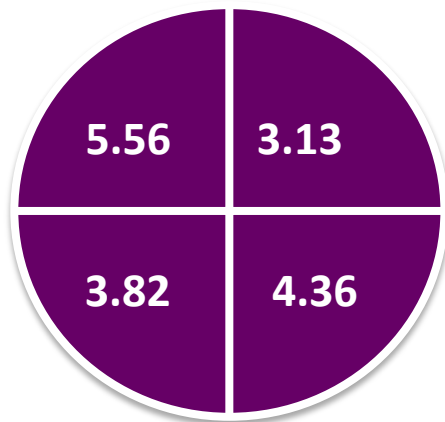
Updrafts + Downdrafts Normalized

*In percent

> $|5 \text{ m s}^{-1}|$

> $|8 \text{ m s}^{-1}|$

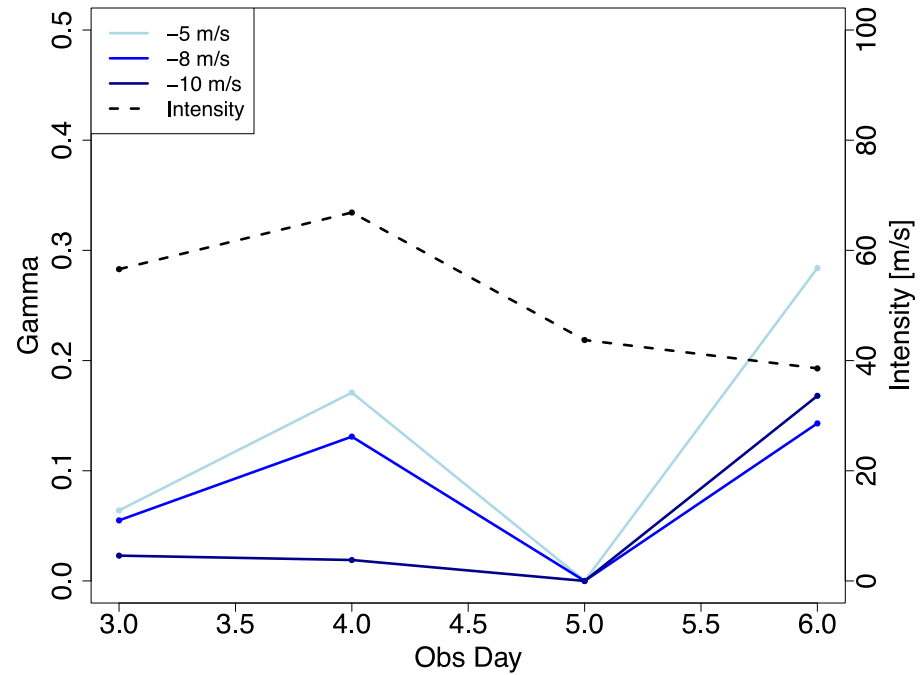
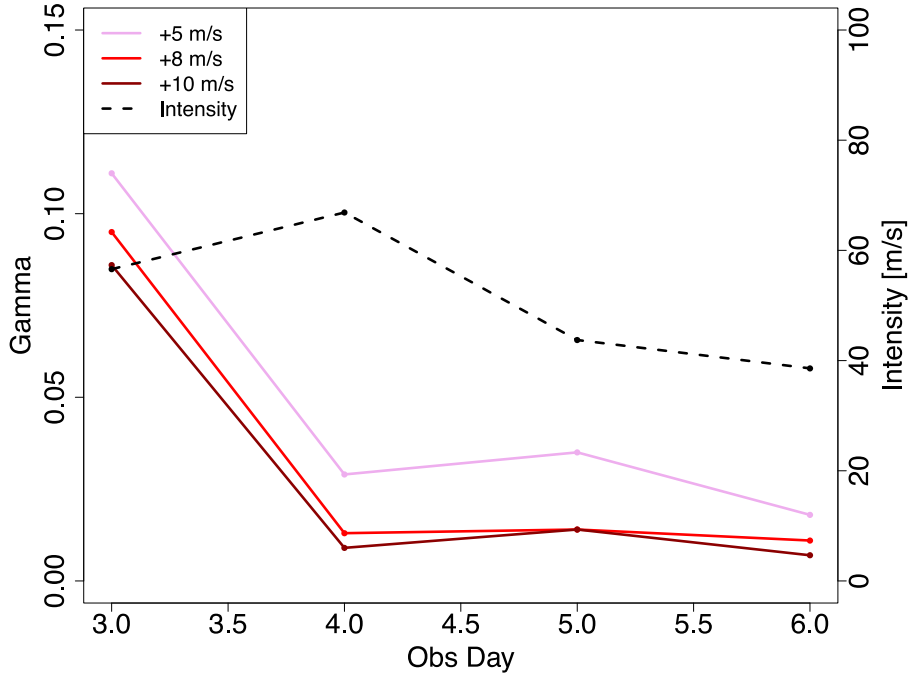
> $|10 \text{ m s}^{-1}|$



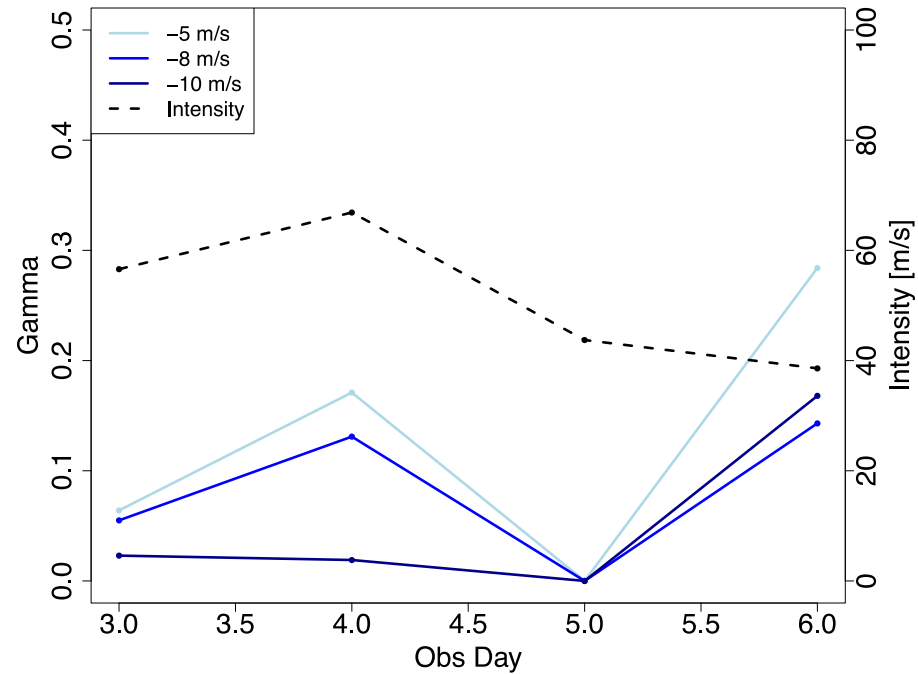
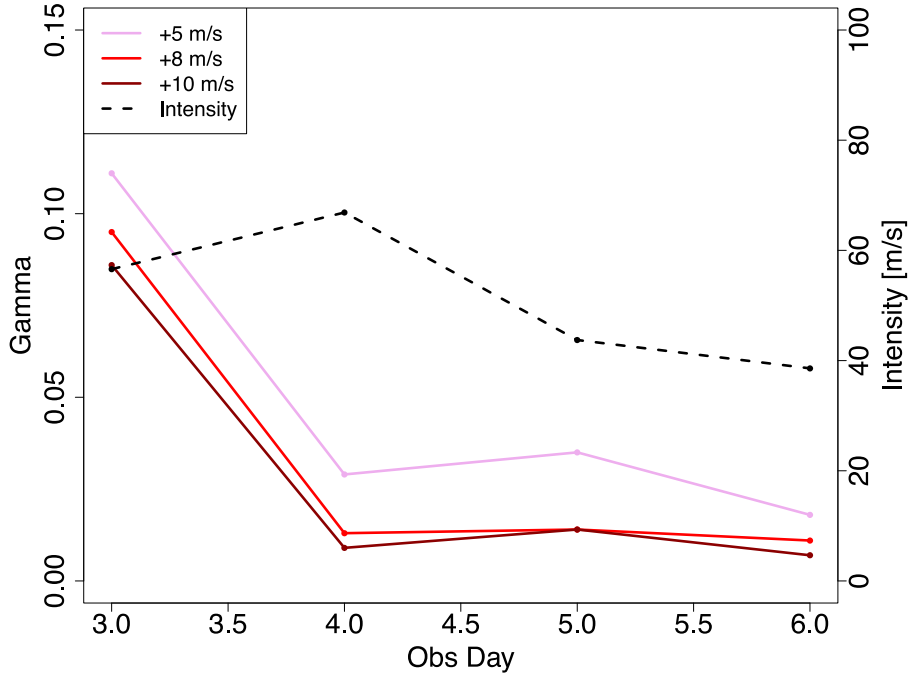
- Most convection in down-shear and left quadrants
 - Preference for DSR in strong UD's...BUT, not what it seems....
 - DSL had more data points further out radially and strength tends to decrease with increasing radii
 - Could also explain peak in percentage CFAzD for USR

Results: Gamma and RMW

Gamma Values

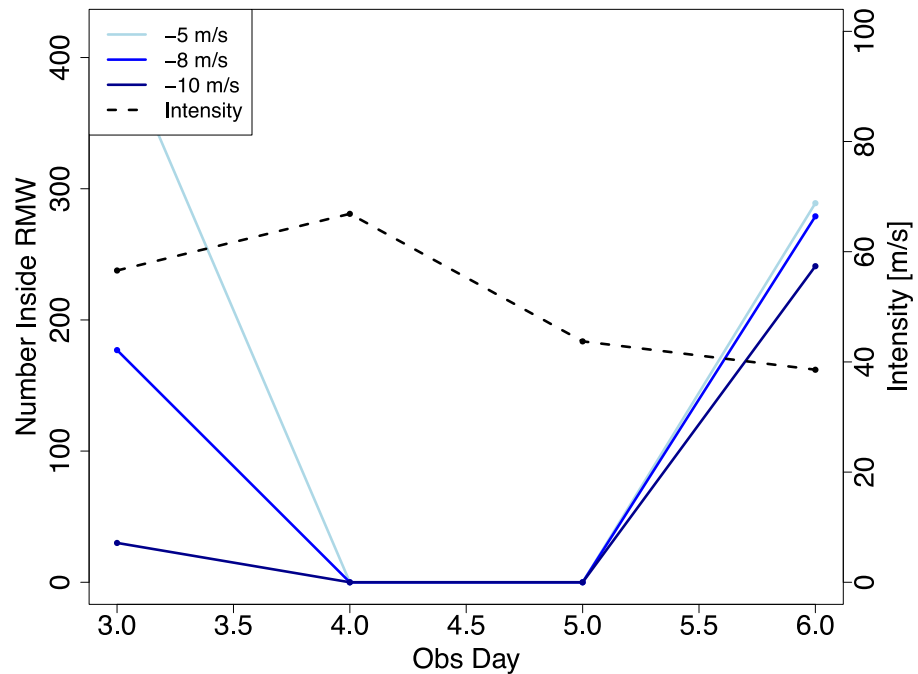
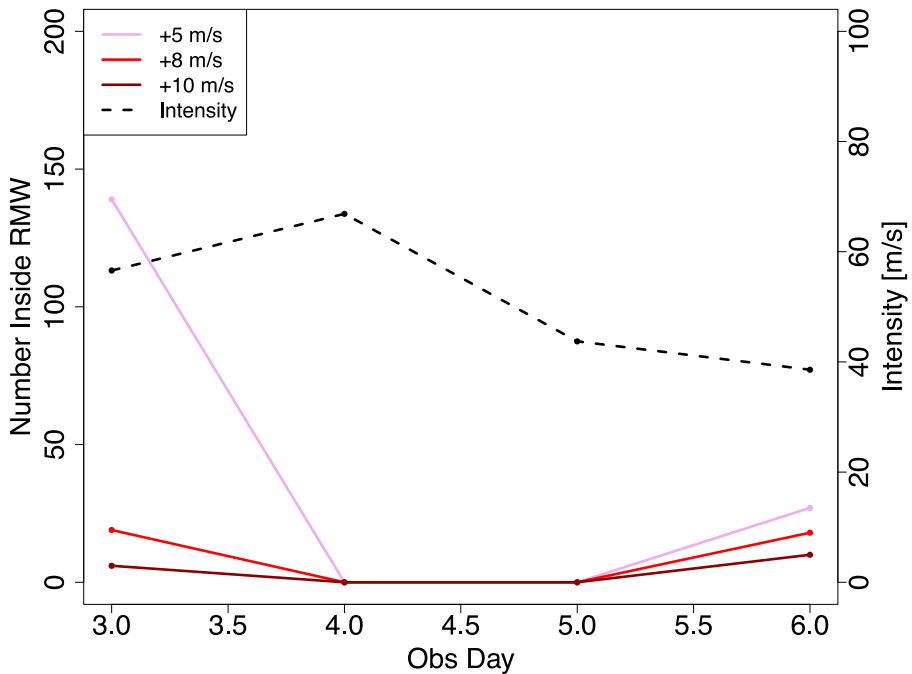


Gamma Values

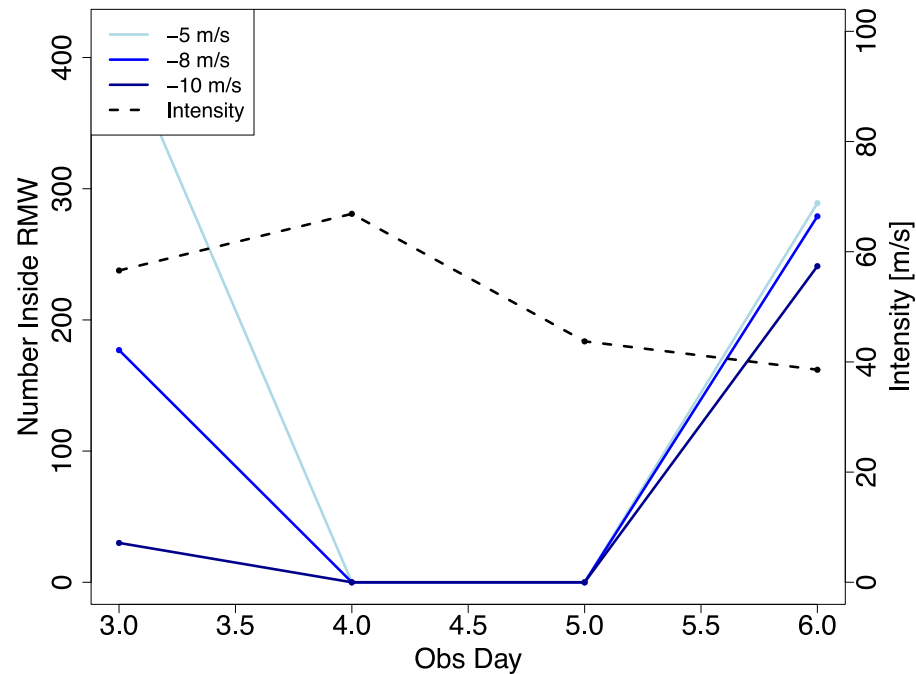
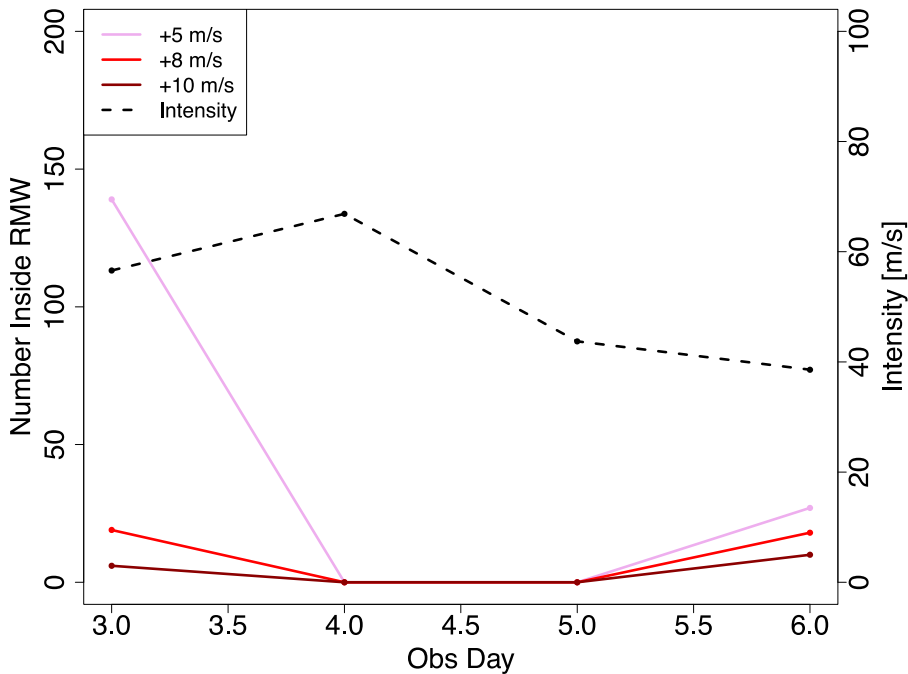


- Gamma tended to maximize for positive thresholds just before intensification
- Gamma tended to maximize for negative thresholds once a TC has hit its peak and begins to decay

Number of UD Data Points Inside RMW



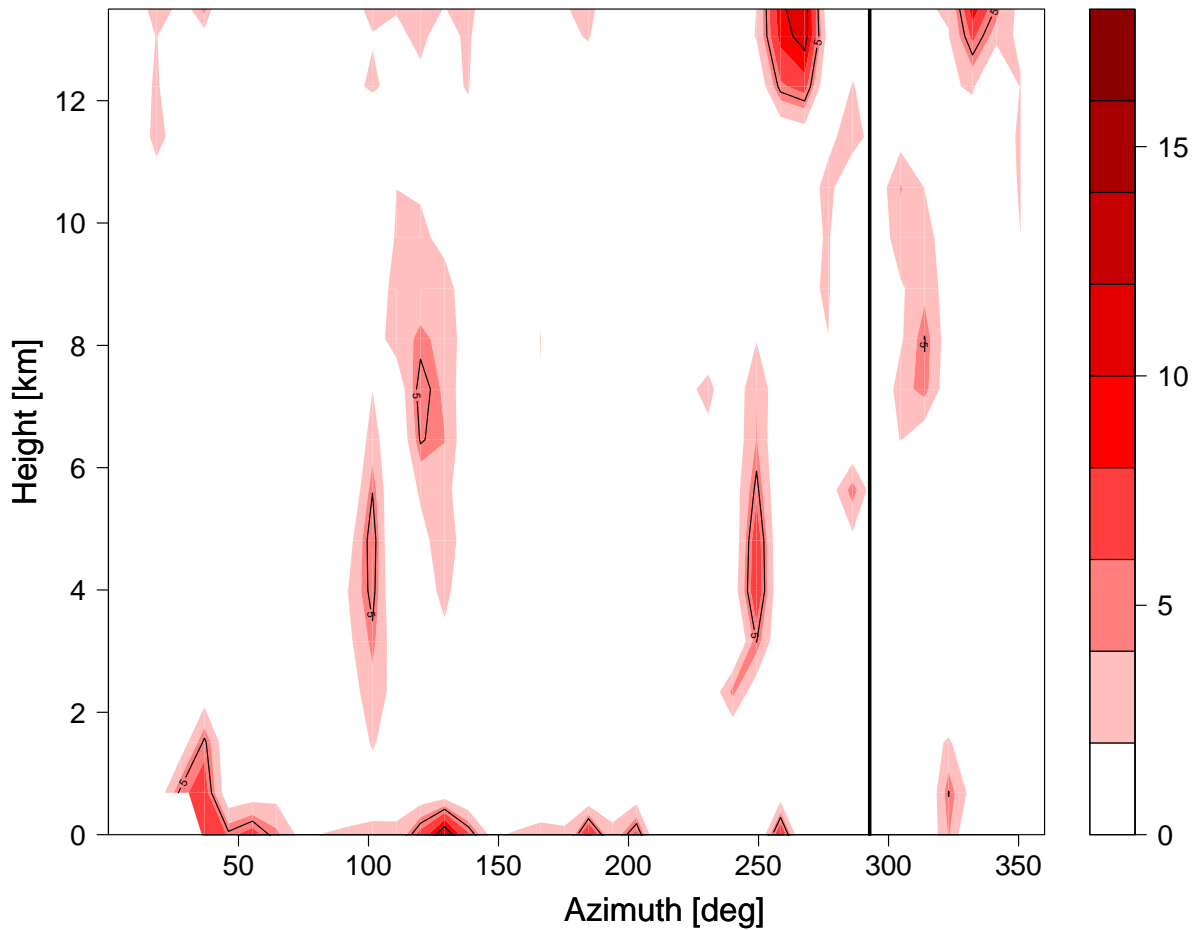
Number of UD Data Points Inside RMW



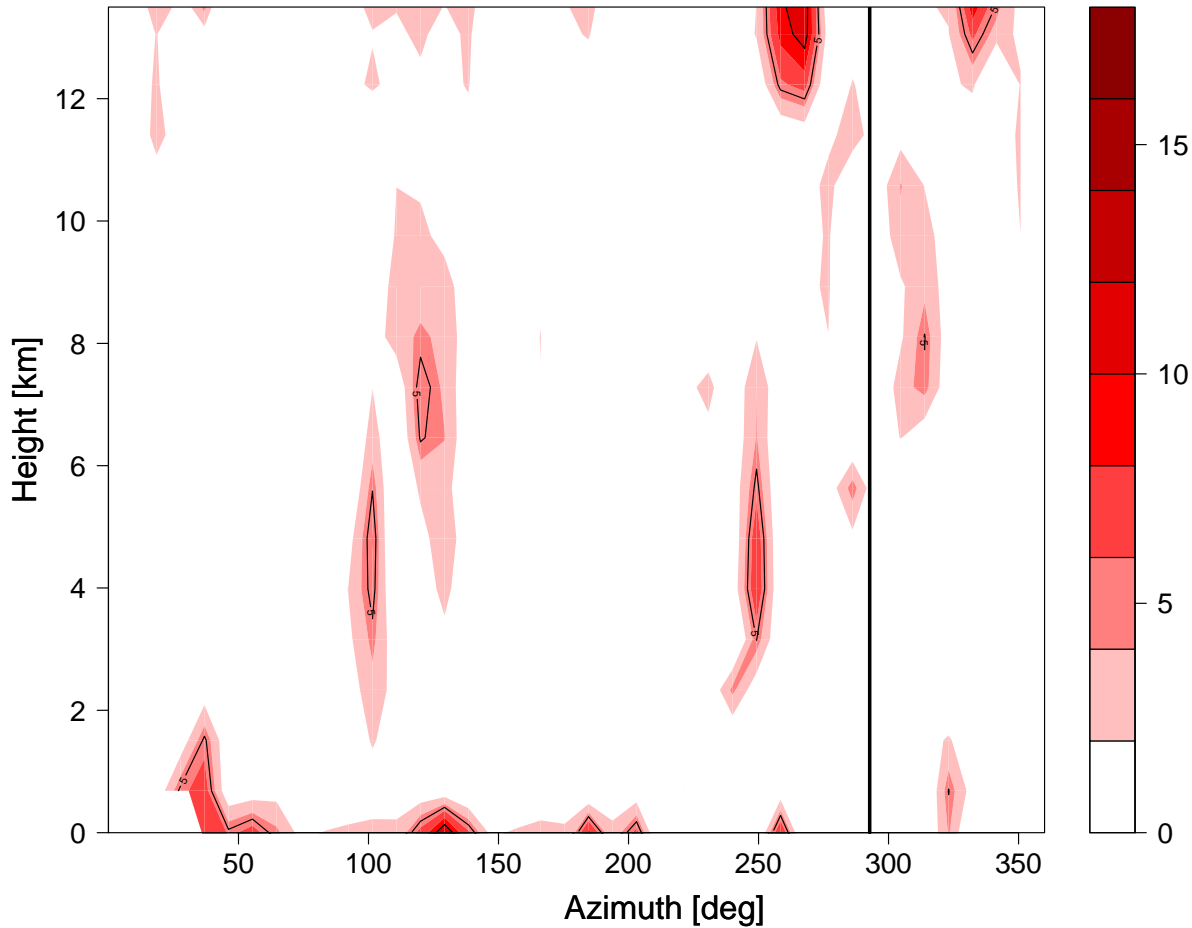
- For both positive and negative thresholds, it appears that there was an increase in convective activity inside the RMW before intensification and it minimized inside the RMW at maximum intensity

Results: Azimuthal and Radial Composites

Azimuthal Composite

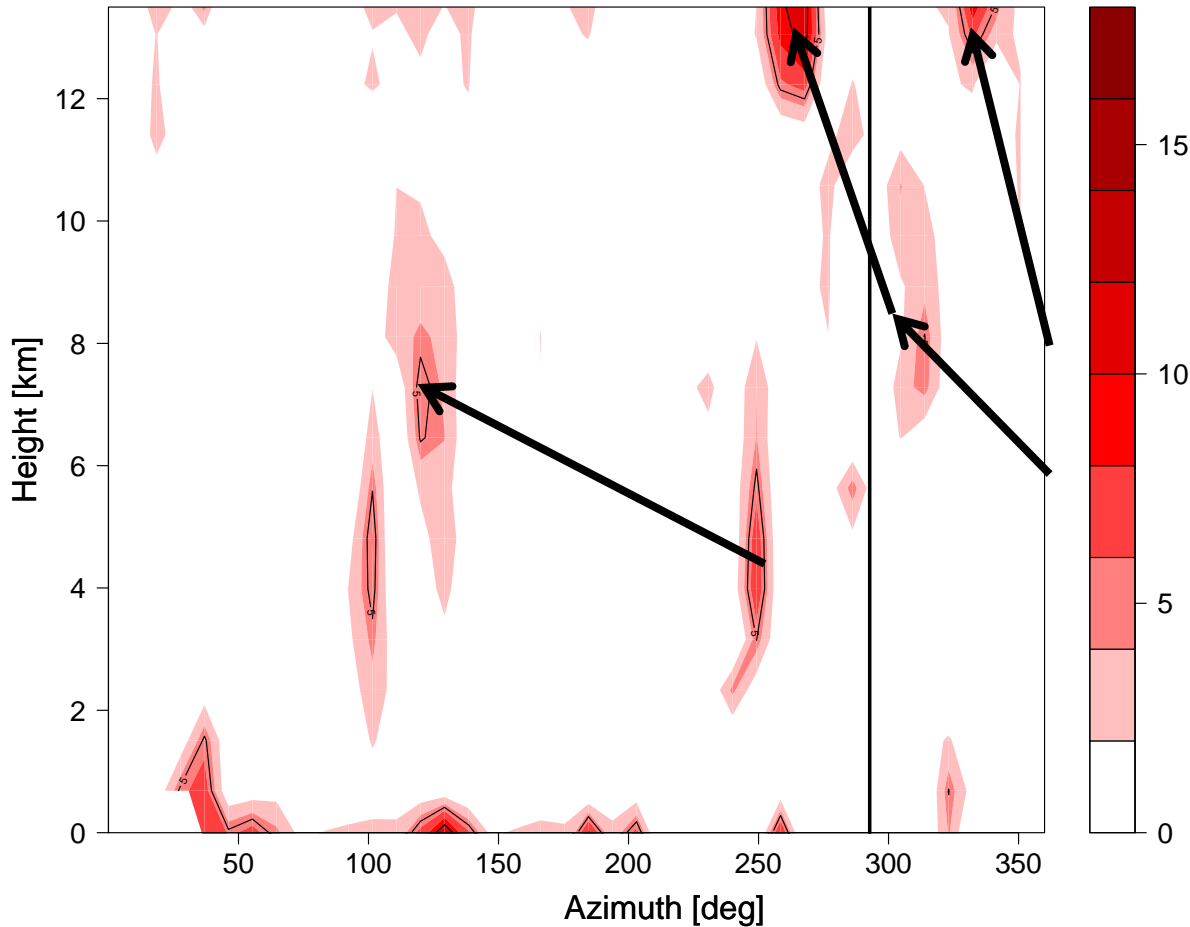


Azimuthal Composite



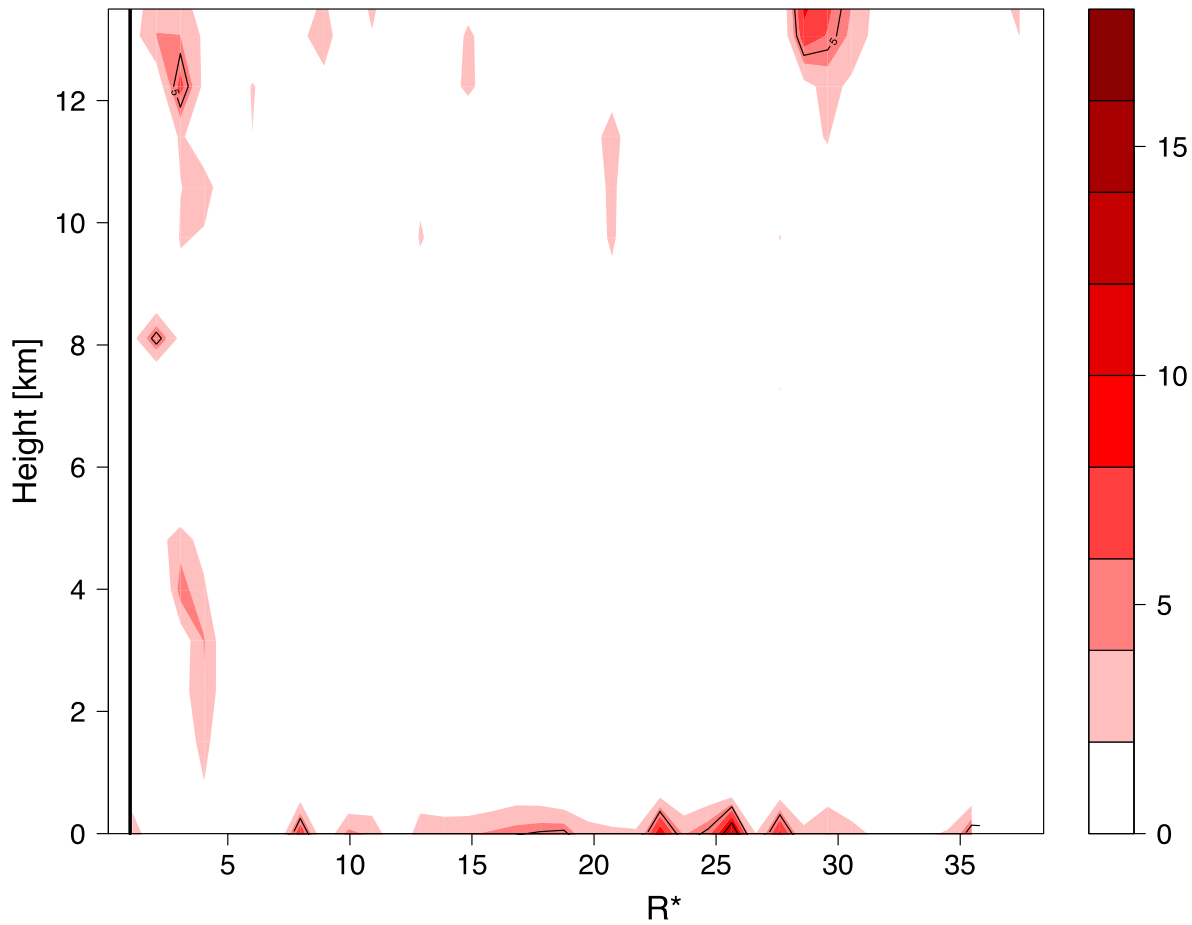
- Evidence of helical rise in updrafts:
 - Initiate in DSR and USR between 50 and 200° AND DSL near 325°
 - Rise and maximize in mid-levels and aloft in the downshear

Azimuthal Composite

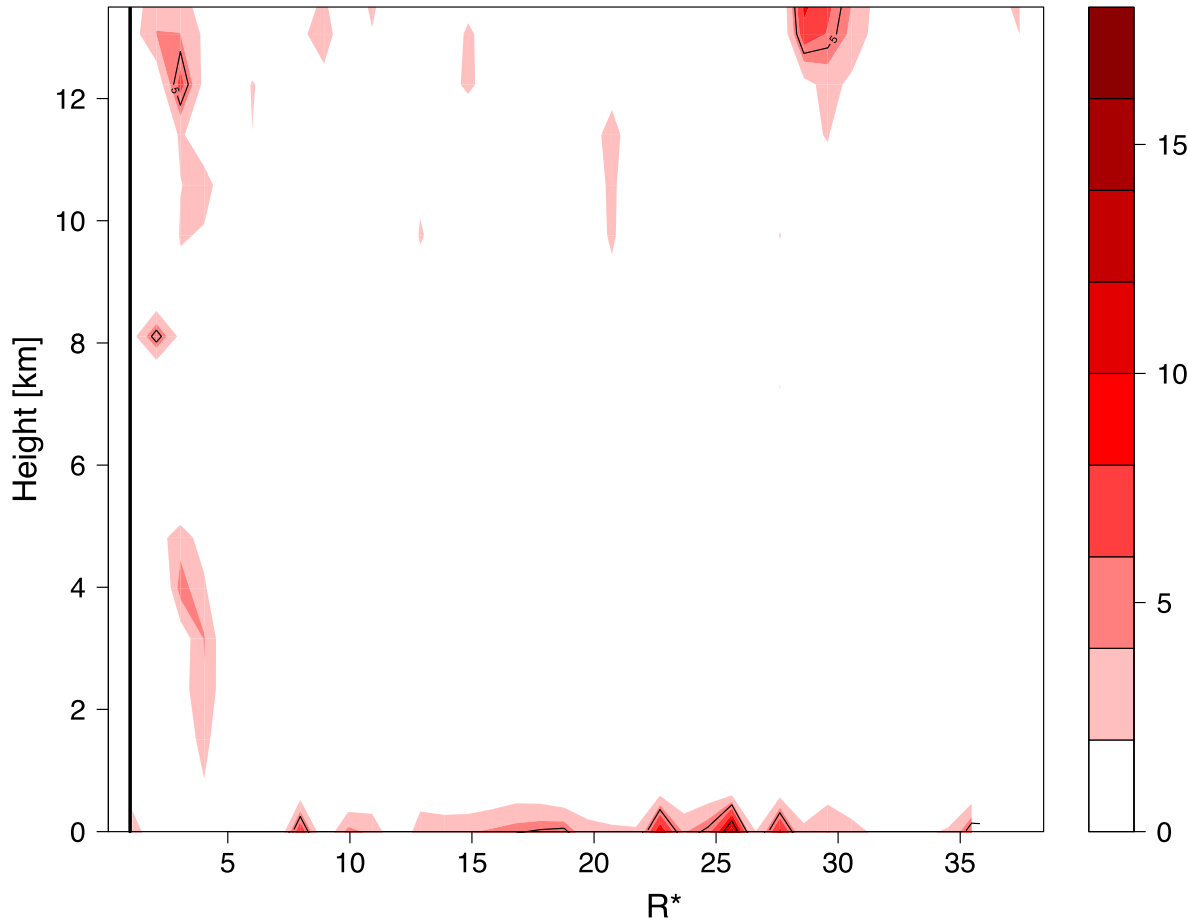


- Evidence of helical rise in updrafts:
 - Initiate in DSR and USR between 50 and 200° AND DSL near 325°
 - Rise and maximize in mid-levels and aloft in the downshear left
 - Unclear as to which surface updrafts rise
 - Need

Radial Composite



Radial Composite



- Inner core updrafts were above 10 km and below 5 km
- Surface based strong updrafts beyond $R^* = 8$
- Upper level updrafts further outward radially at $R^* = 30$
- All outside of RMW

Discussion

- Distinguishing the altitudinal, azimuthal, and radial tendencies for moderate, strong, and extreme UD_s plays a crucial role in:
 - Understanding how shear interacts with TCs
 - TC intensity changes
- Conducted using XDD Dropsondes in Joaquin (2015)
- Extension of Stern et al. (2016) and Stern and Aberson (2006), which only had data in lowest 2 – 3 km
 - Most comparable studies to this current work

Discussion

- Distinguishing the altitudinal, azimuthal, and radial tendencies for moderate, strong, and extreme UD_s plays a crucial role in:
 - Understanding how shear interacts with TCs
 - TC intensity changes
- Conducted using XDD Dropsondes in Joaquin (2015)
- Extension of Stern et al. (2016) and Stern and Aberson (2006), which only had data in lowest 2 – 3 km
 - Most comparable studies to this current work

Discussion

- Distinguishing the altitudinal, azimuthal, and radial tendencies for moderate, strong, and extreme UD_s plays a crucial role in:
 - Understanding how shear interacts with TCs
 - TC intensity changes
- Conducted using XDD Dropsondes in Joaquin (2015)
- Extension of Stern et al. (2016) and Stern and Aberson (2006), which only had data in lowest 2 – 3 km
 - Most comparable studies to this current work

TC Intensity

- Moderate, strong and extreme UD_s occurred in weak and strong TC intensities and in different shear environments
 - Some correlation between convection (via gamma parameter) and intensity
 - Convection tended to increase inside the RMW before intensification

TC Intensity

- Moderate, strong and extreme UD occurred in weak and strong TC intensities and in different shear environments
 - Some correlation between convection (via gamma parameter) and intensity
 - Convection tended to increase inside the RMW before intensification

TC Intensity

- Moderate, strong and extreme UD occurred in weak and strong TC intensities and in different shear environments
 - Some correlation between convection (via gamma parameter) and intensity
 - Convection tended to increase inside the RMW before intensification

UD Locations

- Occurred both inside and outside the RMW, but decreased in strength outside of “inner core”
 - Collectively, majority of UDs were outside of RMW
- Outside of inner core, oscillatory pattern of convection of rainbands
- Vertical velocities maximized:
 - Aloft near 12 km (Jorgensen et al. 1985; Marks et al. 2008; Rogers et al. 2012)
 - Just above the surface (Stern et al. 2016)
- Convection tended to maximize **BROADLY** in the DSL quadrant for UDs (Black et al. 2002; Corbosiero and Molinari 2002, 2003; Stern and Aberson 2006; Guimond et al. 2010; Reasor et al. 2013)
- Suppressed convection in the DSR and USR (between 140 and 180°) quadrants for above moderate UDs

UD Locations

- Occurred both inside and outside the RMW, but decreased in strength outside of “inner core”
 - Collectively, majority of UDs were outside of RMW
- Outside of inner core, oscillatory pattern of convection of rainbands
- Vertical velocities maximized:
 - Aloft near 12 km (Jorgensen et al. 1985; Marks et al. 2008; Rogers et al. 2012)
 - Just above the surface (Stern et al. 2016)
- Convection tended to maximize **BROADLY** in the DSL quadrant for UDs (Black et al. 2002; Corbosiero and Molinari 2002, 2003; Stern and Aberson 2006; Guimond et al. 2010; Reasor et al. 2013)
- Suppressed convection in the DSR and USR (between 140 and 180°) quadrants for above moderate UDs

UD Locations

- Occurred both inside and outside the RMW, but decreased in strength outside of “inner core”
 - Collectively, majority of UDs were outside of RMW
- Outside of inner core, oscillatory pattern of convection of rainbands
- Vertical velocities maximized:
 - Aloft near 12 km (Jorgensen et al. 1985; Marks et al. 2008; Rogers et al. 2012)
 - Just above the surface (Stern et al. 2016)
- Convection tended to maximize **BROADLY** in the DSL quadrant for UDs (Black et al. 2002; Corbosiero and Molinari 2002, 2003; Stern and Aberson 2006; Guimond et al. 2010; Reasor et al. 2013)
- Suppressed convection in the DSR and USR (between 140 and 180°) quadrants for above moderate UDs

UD Locations

- Occurred both inside and outside the RMW, but decreased in strength outside of “inner core”
 - Collectively, majority of UDs were outside of RMW
- Outside of inner core, oscillatory pattern of convection of rainbands
- Vertical velocities maximized:
 - Aloft near 12 km (Jorgensen et al. 1985; Marks et al. 2008; Rogers et al. 2012)
 - Just above the surface (Stern et al. 2016)
- Convection tended to maximize **BROADLY** in the DSL quadrant for UDs (Black et al. 2002; Corbosiero and Molinari 2002, 2003; Stern and Aberson 2006; Guimond et al. 2010; Reasor et al. 2013)
- Suppressed convection in the DSR and USR (between 140 and 180°) quadrants for above moderate UDs

UD Locations

- Occurred both inside and outside the RMW, but decreased in strength outside of “inner core”
 - Collectively, majority of UD's were outside of RMW
- Outside of inner core, oscillatory pattern of convection of rainbands
- Vertical velocities maximized:
 - Aloft near 12 km (Jorgensen et al. 1985; Marks et al. 2008; Rogers et al. 2012)
 - Just above the surface (Stern et al. 2016)
- Convection tended to maximize **BROADLY** in the DSL quadrant for UD's (Black et al. 2002; Corbosiero and Molinari 2002, 2003; Stern and Aberson 2006; Guimond et al. 2010; Reasor et al. 2013)
- Suppressed convection in the DSR and USR (between 140 and 180°) quadrants for above moderate UD's

Composite Plots

- Radial composite plot showed evidence of inner core convection maximizing aloft
- Outside of the inner core, surface updrafts increased in strength
- Azimuthal composite plots show strong surface updrafts rising helically
 - Location of initiation variable
 - DSR/USR and DSL
 - Combining inner core and rainband regions may be an issue

Composite Plots

- Radial composite plot showed evidence of inner core convection maximizing aloft
- Outside of the inner core, surface updrafts increased in strength
- Azimuthal composite plots show strong surface updrafts rising helically
 - Location of initiation variable
 - DSR/USR and DSL
 - Combining inner core and rainband regions may be an issue

Composite Plots

- Radial composite plot showed evidence of inner core convection maximizing aloft
- Outside of the inner core, surface updrafts increased in strength
- Azimuthal composite plots show strong surface updrafts rising helically
 - Location of initiation variable
 - DSR/USR and DSL
 - Combining inner core and rainband regions may be an issue

Future Work

- Examine the sources of these moderate, strong and extreme UDAs
 - 37 GHz polarization correction temperature microwave data and satellite data (Naval Research Laboratory)
 - Moisture and buoyancy
 - Bulk Richardson number
 - CAPE
 - Sea surface temperature
 - Potentially, modeling initialized on soundings
- Differentiating between inner core convection and inner rainband convection
- Evaluate the strength of the updraft cores in relation to the secondary circulation

Future Work

- Examine the sources of these moderate, strong and extreme UDAs
 - 37 GHz polarization correction temperature microwave data and satellite data (Naval Research Laboratory)
 - Moisture and buoyancy
 - Bulk Richardson number
 - CAPE
 - Sea surface temperature
 - Potentially, modeling initialized on soundings
- Differentiating between inner core convection and inner rainband convection
- Evaluate the strength of the updraft cores in relation to the secondary circulation

Future Work

- Examine the sources of these moderate, strong and extreme UDAs
 - 37 GHz polarization correction temperature microwave data and satellite data (Naval Research Laboratory)
 - Moisture and buoyancy
 - Bulk Richardson number
 - CAPE
 - Sea surface temperature
 - Potentially, modeling initialized on soundings
- Differentiating between inner core convection and inner rainband convection
- Evaluate the strength of the updraft cores in relation to the secondary circulation

Conclusions

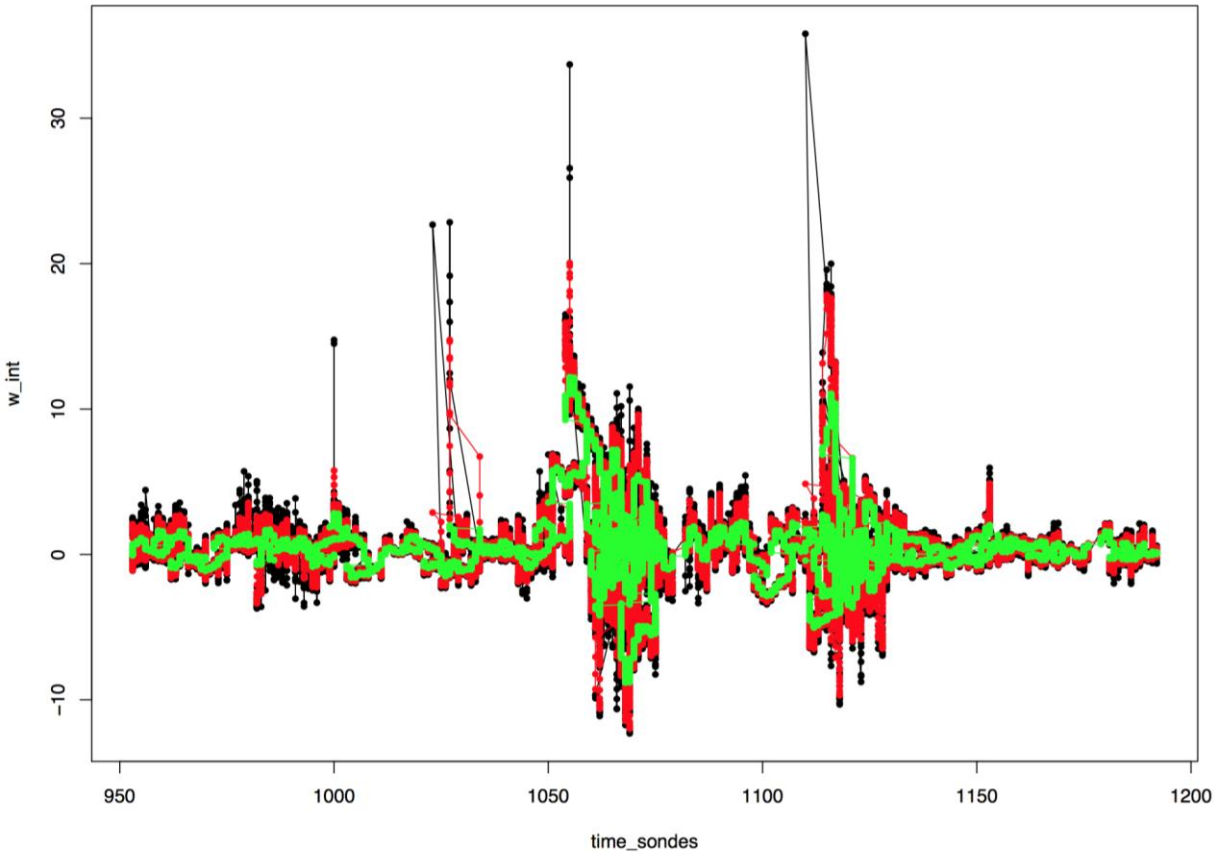
- UDs occurred in throughout Joaquin regardless of intensity or shear strength
- Occurred both inside and outside RMW
 - Inside RMW maximum before intensification
- DSL convective preference
- Suppression in parts of the USR and DSR
- UD strength maximized aloft
- Helically rising updrafts

References

- Black, M. L., J. F. Gamache, F. D. M. Jr., C. E. Samsury, and H. E. Willoughby, 2002: Eastern Pacific Hurricanes Jimena of 1991 and Olivia of 1994: The effect of vertical shear on structure and intensity. *Mon. Wea. Rev.*, **130**, 2291–2312.
- Black, P., L. Harrison, M. Beaubien, R. Bluth, R. Woods, A. Penny, R. Smith, and J. Doyle, 2016: High Definition Sounding System (HDSS) for atmospheric profiling. *J. Atmos. Oceanic Technol.*, in press, doi:10.1175/JTECH-D-14-00210.1.
- Corbosiero, K. L., and J. Molinari, 2002: The effects of vertical wind shear on the distribution of convection in tropical cyclones. *Mon. Wea. Rev.*, **130**, 2110–2123.
- Corbosiero, K. L., and J. Molinari, 2003: The relationship between storm motion, vertical wind shear, and convective asymmetries in tropical cyclones. *J. Atmos. Sci.*, **60**, 366–376.
- DeMaria, M., and J. Kaplan, 1994: A statistical hurricane intensity prediction scheme (SHIPS) for the Atlantic basin. *Wea. Forecasting*, **9**, 209–220.
- Guimond, S. R., G. M. Heymsfield, and F. J. Turk, 2010: Multiscale observations of Hurricane Dennis (2005): The effects of hot towers on rapid intensification. *J. Atmos. Sci.*, **67**, 633–654, doi:10.1175/2009JAS3119.1.
- Hock, T. F., and J. L. Franklin, 1999: The NCAR GPS dropwindsonde. *Bull. Amer. Meteor. Soc.*, **80**, 407–420.
- Jorgensen, D. P., E. J. Zipser, and M. A. LeMone, 1985: Vertical motions in intense hurricanes. *J. Atmos. Sci.*, **42**, 839–856.
- Marks, F. D., P. G. Black, M. T. Montgomery, and R. W. Burpee, 2008: Structure of the eye and eyewall of Hurricane Hugo (1989). *Mon. Weather Rev.*, **136**, 1237–1259.
- Reasor, P. D., R. Rogers, and S. Lorsolo, 2013: Environmental flow impacts on tropical cyclone structure diagnosed from airborne Doppler radar composites. *Mon. Wea. Rev.*, **141**, 2949–2969, doi:10.1175/MWR-D-12-00334.1.
- Rogers, R., S. Lorsolo, P. Reasor, J. Gamache, and F. Marks, 2012: Multiscale analysis of tropical cyclone kinematic structure from airborne Doppler radar composites. *Mon. Wea. Rev.*, **140**, 77–99, doi:10.1175/MWR-D-10-05075.1.
- Stern, D. P., and S. D. Abersson, 2006: Extreme vertical winds measured by dropwindsondes in hurricanes. *27th Conf. on Hurricanes and Tropical Meteorology*.
- Stern, D. P., G. H. Bryan, and S. D. Abersson, 2016: Extreme low-level updrafts and wind speeds measured by dropsondes in tropical cyclones. *Mon. Wea. Rev.*, **144**, 2177–2204, doi:10.1175/MWR-D-15-0313.1.

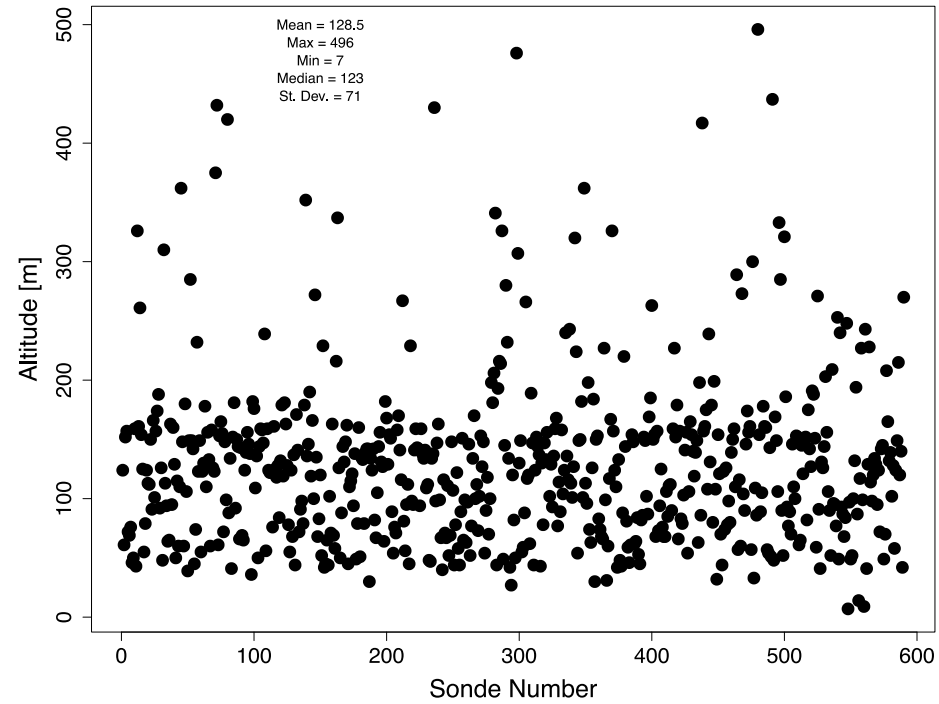
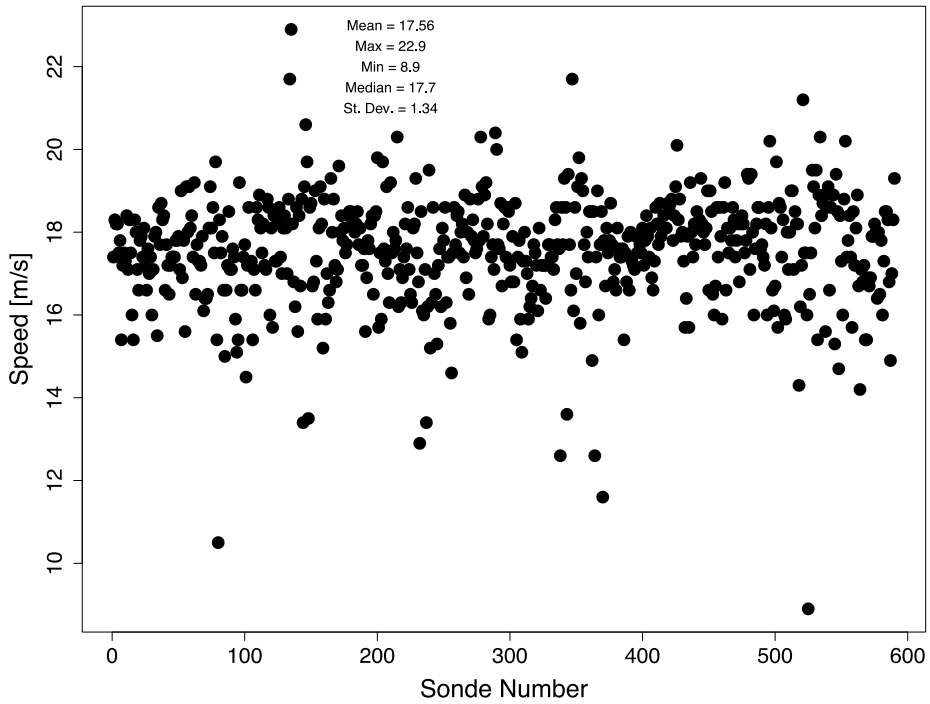
Bonus Slides

Filtered Data Example

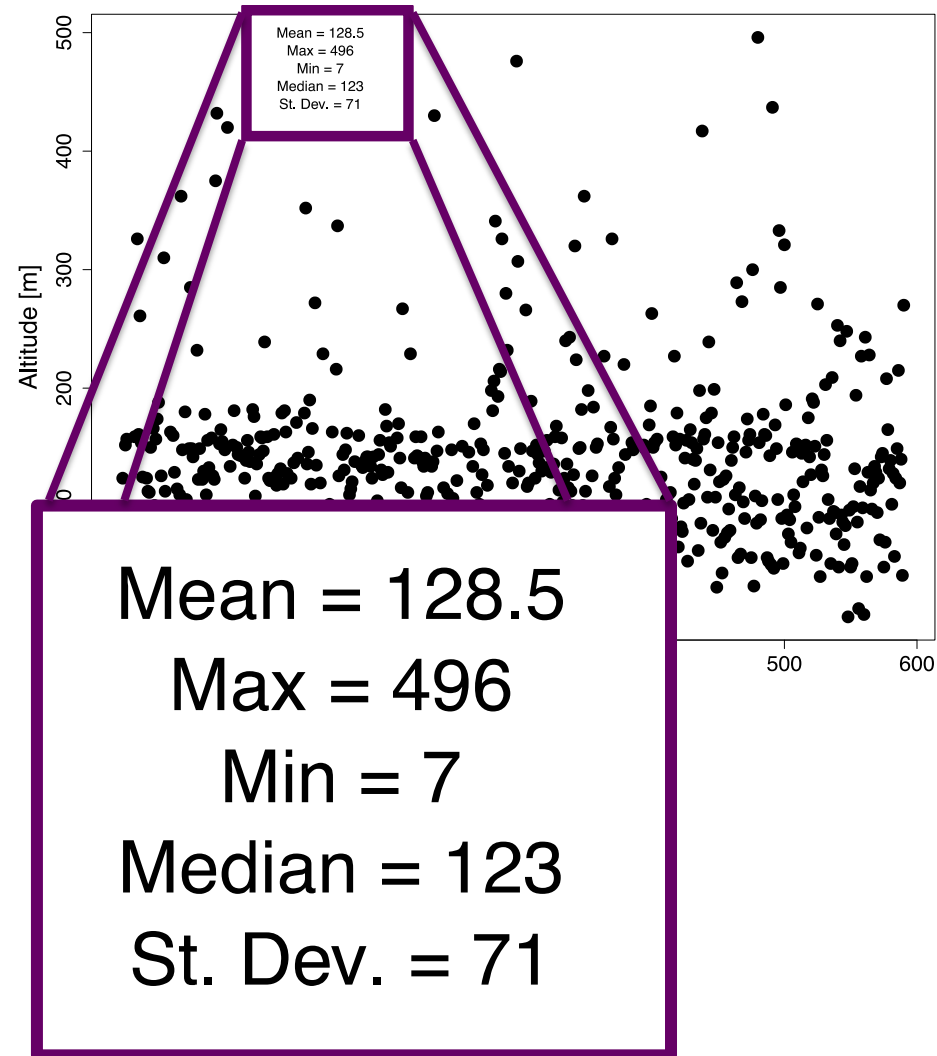
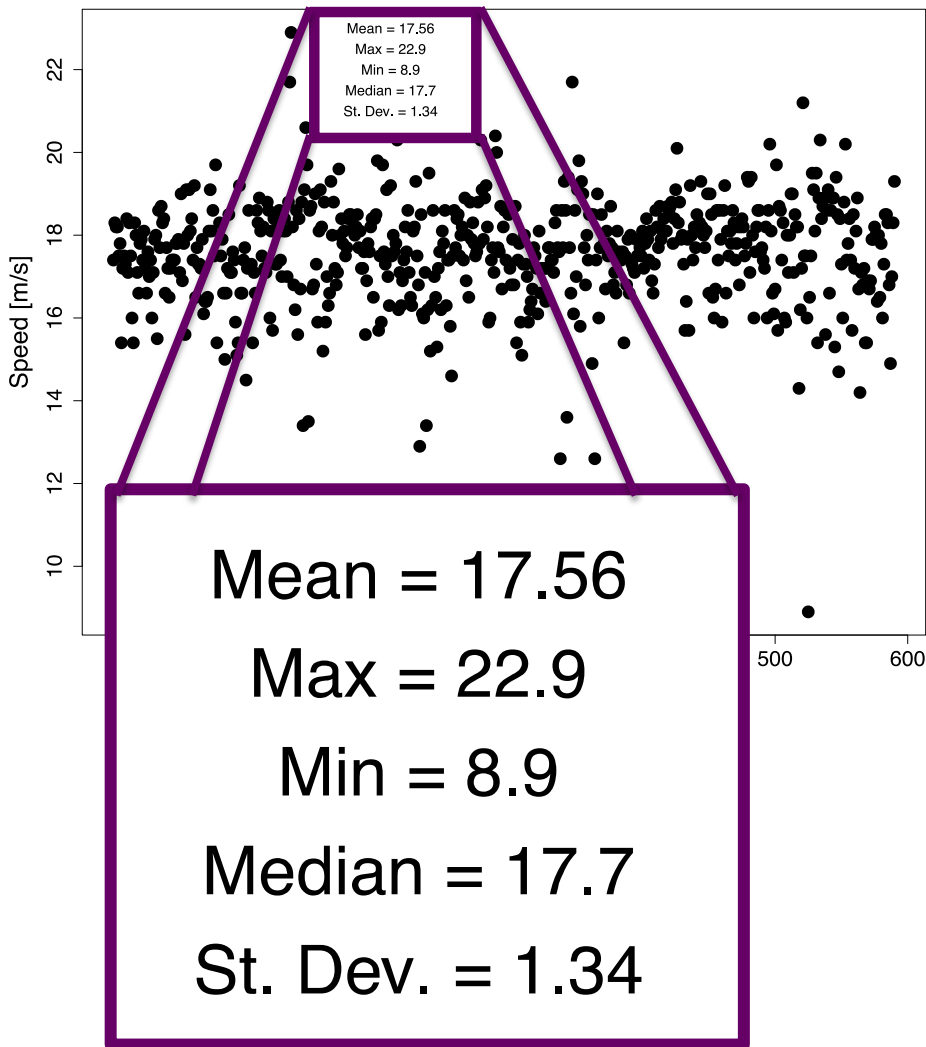


- Example of filtering of data: Joaquin on 02 Oct. 2015
- Black is raw data
- Red is nine-point binomial filter
- Green is 100 Hz Butter filter that has been corrected for phase shift

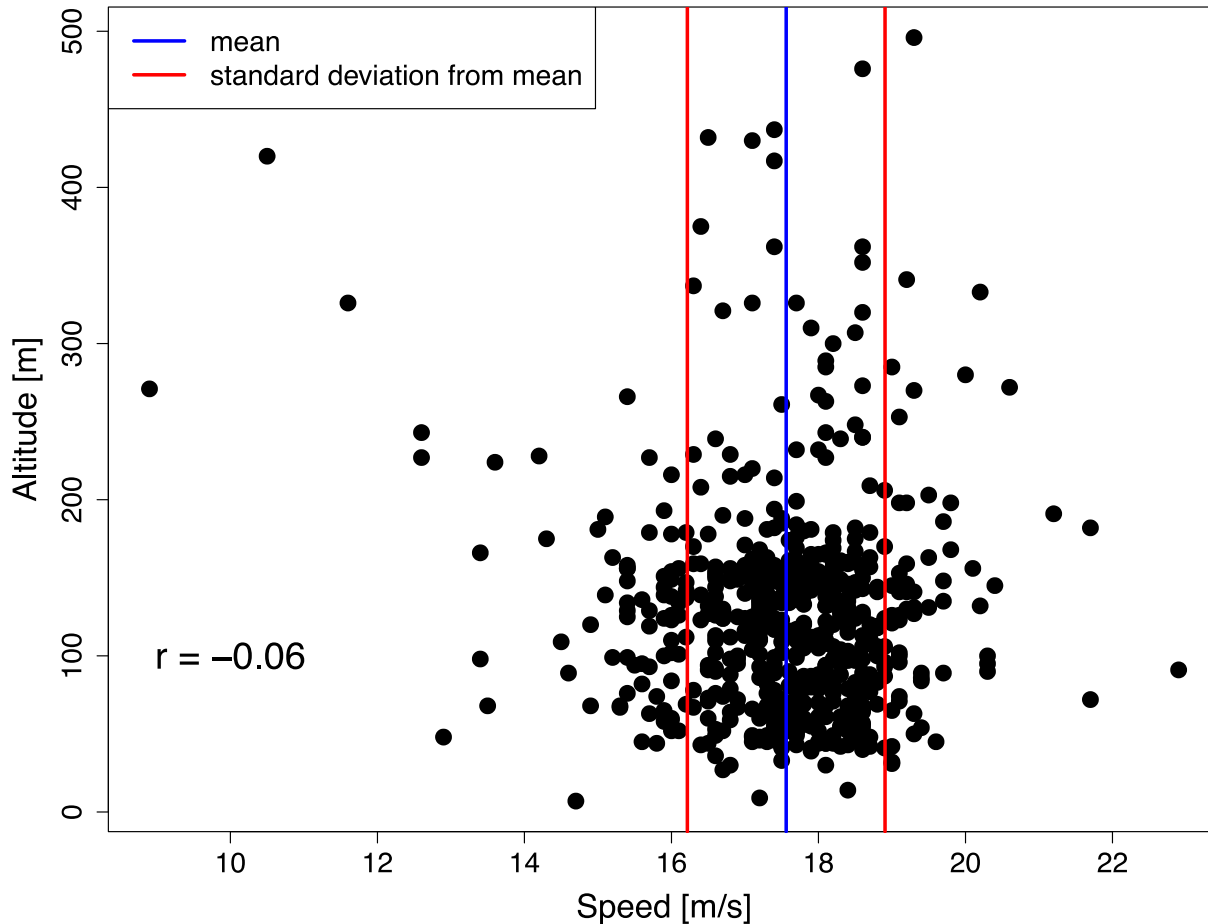
Surface Fall Speed Factor



Surface Fall Speed Factor



Surface Fall Speed Factor



- Very weak (and negative) correlation between height of “surface” and the fall speed
- Most data within 1 standard deviation of mean fall speed
- Outside of 1 standard deviation not affected by altitude
- Close to the 18 m s^{-1} surface fall speed reported by Black et al. (2016)